PTEP

Prog. Theor. Exp. Phys. **2017**, 053B01 (34 pages)
DOI: 10.1093/ptep/ptx047

Non-Abelian gauge field localization on walls and geometric Higgs mechanism

Masato Arai[1], Filip Blaschke[2,*], Minoru Eto[3], and Norisuke Sakai[4]

[1] *Faculty of Science, Yamagata University, Kojirakawa-machi 1-4-12, Yamagata, Yamagata 990-8560, Japan*
[2] *Faculty of Philosophy and Science, Silesian University in Opava, Bezručovo nám. 1150/13, 746 01 Opava, Czech Republic*
[3] *Department of Physics, Yamagata University, Kojirakawa-machi 1-4-12, Yamagata, Yamagata 990-8560, Japan*
[4] *Department of Physics, and Research and Education Center for Natural Sciences, Keio University, 4-1-1 Hiyoshi, Yokohama, Kanagawa 223-8521, Japan*
*E-mail: fblasch@post.cz

Received March 16, 2017; Accepted March 28, 2017; Published May 5, 2017

Combining the semiclassical localization mechanism for gauge fields with N domain wall background in a simple SU(N) gauge theory in 5 space-time dimensions, we investigate the geometric Higgs mechanism, where a spontaneous breakdown of the gauge symmetry comes from splitting of domain walls. The mass spectra are investigated in detail for the phenomenologically interesting case SU(5) $\rightarrow$ SU(3) $\times$ SU(2) $\times$ U(1), which is realized on a split configuration of coincident triplet and doublet of domain walls. We derive a low-energy effective theory in a generic background using the moduli approximation, where all nonlinear interactions between effective fields are captured up to 2 derivatives. We observe novel similarities between domain walls in our model and D-branes in superstring theories.

Subject Index B33, B35, B40, B42, B43

1. Introduction

One of the most puzzling features of the Standard Model (SM) is the lack of explanation of the gauge hierarchy problem. To solve this problem, apart from other popular ideas such as supersymmetry (Refs. [1–4]) and composite (Technicolor) models (Refs. [5,6]), the brane-world scenario has been invoked in various forms (Refs. [7–11]).

The possibility of dynamical realization of the brane-world idea via a domain wall was recognized quite early (Ref. [12]). A long-lasting obstacle to serious investigations of brane-world scenarios by domain walls, however, was the localization of gauge fields. Naive attempts to localize gauge fields on the domain wall with the Higgs phase in the bulk give no massless gauge fields in the effective theory (Refs. [7,13,14]; see also Refs. [15–18] for related studies). The so-called Dvali–Shifman (DS) mechanism (Ref. [13]) is a popular way to get around the problem, inspired by a nonperturbative feature of non-Abelian gauge theories—the confinement. However, it has not been proven whether non-Abelian gauge theories that exhibit the confinement in the bulk exist in $(d+1)$-dimensional space-time with $d \geq 4$.

It was pointed out in Ref. [19] that one can implement the gauge field localization more easily in a semiclassical way. If the gauge coupling depends on the extra-dimensional coordinate in such a way that it rapidly diverges away from the brane (semiclassical picture of confinement) while remaining

Funded by SCOAP[3]

finite in the vicinity of the brane, it effectively provides a confining vacuum for zero modes of gauge fields with the 4-dimensional gauge invariance intact. The mechanism is realized by a field-dependent gauge kinetic term (Ref. [19]). This arises naturally in $\mathcal{N} = 2$ supersymmetric gauge theories in 5 space-time dimensions in the form of the so-called prepotential (Refs. [20,21]). In this framework, we have constructed models of non-Abelian gauge fields localized around domain walls and worked out nonlinear interactions of moduli fields (Refs. [22,23]).

In this paper, we investigate the Higgs mechanism caused by the domain walls. In the previous works Refs. [22,23] our studies were focused on how to localize the massless non-Abelian gauge fields on the walls. In contrast, in the present paper, we aim to figure out how the massless gauge fields get nonzero masses in the framework (Refs. [19,22,23]). Either by the DS or the Ohta–Sakai (OS) mechanism, the localization of non-Abelian gauge fields occurs due to the confining phase in the bulk. This has many similarities with the localization of gauge fields on D-branes in superstring theories. Indeed, we found in our previous works Refs. [22,23] that N coincident domain walls are needed to have massless $SU(N)$ gauge fields inside the domain walls. Therefore, we naturally expect that the Higgs mechanism also goes similarly to low-energy effective theory on D-branes, and we will show it is indeed so.

It is often the case that a non-Abelian global symmetry is realized in the coincident wall configuration. It has been found previously that the splitting of domain walls can break the global symmetry, and the moduli fields corresponding to the wall positions become massless Nambu–Goldstone (NG) bosons associated to the symmetry breaking (Refs. [24,25]). When non-Abelian gauge fields couple to the global symmetry, one naively expects that they will absorb these moduli fields and become massive. If this is the case, a splitting of positions of domain walls in the 5-dimensional theory can induce a spontaneous breakdown of non-Abelian gauge symmetry in the effective theory on domain walls. In other words, the moduli fields corresponding to the wall positions play the role of the Higgs field in the effective field theory. Since the geometrical data such as wall positions provide scalar fields realizing the Higgs phenomenon, we call this mechanism the *geometric Higgs mechanism*.

In our previous works, we have observed the geometric Higgs mechanism (Refs. [22,23]) indirectly through the effective Lagrangian. The purpose of this paper is to directly study the geometric Higgs mechanism from the 5-dimensional point of view in detail. Since the would-be NGs are not homogeneously distributed, as they are affected by the domain wall background, the geometric Higgs mechanism is not as straightforward as the standard Higgs mechanism in a homogeneous Higgs vacuum. We will study the physical spectrum via mode equations for all fields in detail and show that the gauge fields associated with the broken gauge symmetry absorb the localized NGs and get nonzero masses.

Furthermore, we calculate the 4-dimensional low-energy effective Lagrangian in an arbitrary domain wall background in the so-called moduli approximation (Ref. [26]). This effective Lagrangian captures full nonlinear interactions between moduli fields up to 2 derivative terms, which we write in a closed form. With the effective Lagrangian, we give a proof of the geometric Higgs mechanism from the perspective of low-energy effective theory on the domain walls.

Last, many similarities between domain walls and D-branes have been shown in the literature. For example, in Refs. [27–36] a D1–D3-like configuration was found. Furthermore, the low-energy effective theory on domain walls was found to be similar to that on D-branes (Refs. [37–39,46]). In our work, we find new evidence for the correspondence between domain walls and D-branes. Like in D-branes, the number of coincident domain walls determines the rank of the gauge group. In addition, the masses of gauge bosons are proportional to the distance between walls, at least when they are close. As a result, our model further strengthens the notion of domain-wall–D-brane correspondence.

The paper is organized as follows. In Sect. 2 we present an $\mathrm{SU}(N)$ gauge theory with 2 adjoint scalar fields. In Sect. 3 we construct N domain walls and discuss the ungauged fluctuation spectrum. In Sect. 4 we turn on the gauge interactions and analyze the spectrum of fluctuations around the 3–2 split background in the $N = 5$ model to demonstrate the geometric Higgs mechanism. Section 5 is devoted to the low-energy effective Lagrangian in 4 dimensions with the moduli approximation. Last, Sect. 6 is devoted to a summary and future prospects. In Appendix A we present the Kaluza–Klein spectrum of the Abelian-Higgs model on $\mathbb{R}^{3,1} \times S^1/Z_2$, which we consider as a toy model to our theory, while in Appendix B we have collected several identities useful to compute the effective Lagrangian.

2. The model

Let us consider a (4+1)-dimensional $\mathrm{SU}(N)$ gauge theory with 2 adjoint scalars $\hat{T}$ and $\hat{S}$ transforming as $\hat{T} \to U_N \hat{T} U_N^\dagger$ and $\hat{S} \to U_N \hat{S} U_N^\dagger$ with $U_N \in \mathrm{SU}(N)$, and 2 singlets T^0 and S^0. We combine both adjoints and singlets into Hermitian $N \times N$ matrices $T \equiv \hat{T} + \mathbf{1}_N \frac{T^0}{N}$ and $S \equiv \hat{S} + \mathbf{1}_N \frac{S^0}{N}$. The Lagrangian is given as

$$\mathcal{L} = \mathcal{L}_{\mathrm{B}} + \mathcal{L}_{\mathrm{OS}}. \tag{2.1}$$

The first part $\mathcal{L}_{\mathrm{B}}$ contains kinetic and potential terms for bosons except for the $\mathrm{SU}(N)$ gauge kinetic term as

$$\mathcal{L}_{\mathrm{B}} = \mathrm{Tr}\big[D_M T D^M T + D_M S D^M S\big] - V, \tag{2.2}$$

$$V = \mathrm{Tr}\Big[\lambda^2\big(v^2 \mathbf{1}_N - T^2 - S^2\big)^2 + \Omega^2 S^2 - \xi\big[T, S\big]^2\Big], \tag{2.3}$$

where λ and ξ are coupling constants and where Ω is a mass parameter for S. We use mostly negative metric signature. The covariant derivatives are defined by

$$D_M T = \partial_M T + i\big[A_M, T\big], \qquad D_M S = \partial_M S + i\big[A_M, S\big]. \tag{2.4}$$

The potential (2.3) is chosen not for its generality, but rather to ensure analytic solutions for both the background solution and most of the fluctuation spectra. This will help in subsequent sections to keep the discussion as simple as possible, without sacrificing the generality of our results as more generic potentials than (2.3) would make no qualitative difference.

The field-dependent gauge kinetic term $\mathcal{L}_{\mathrm{OS}}$ is given in the form

$$\mathcal{L}_{\mathrm{OS}} = -\,\mathrm{Tr}\big[F(S) G_{MN} G^{MN}\big], \tag{2.5}$$

where $F(S)$ is an arbitrary polynomial function of S, and $G_{MN} = \partial_M A_N - \partial_N A_M + i\big[A_M, A_N\big]$ is the field strength of $\mathrm{SU}(N)$ gauge fields. The gauge transformation is defined by $A_\mu \to U_N A_\mu U_N^\dagger + i\partial_\mu U_N U_N^\dagger$. The field-dependent gauge coupling term $\mathcal{L}_{\mathrm{OS}}$ is responsible for localization of gauge fields on the world-volume of domain walls in the background T and S fields. In the original work Ref. [19], the function F is restricted to be a linear function by the supersymmetry, but in this work we do not impose supersymmetry and, for convenience, we take

$$F(S) = aS^2, \tag{2.6}$$

Table 1. The mass dimensions of the fields and parameters.

Fields and parameters	A_M	T	S	Ω	λ	v	$\bar{v}$	ξ	a
Mass dimension	1	$\frac{3}{2}$	$\frac{3}{2}$	1	$-\frac{1}{2}$	$\frac{3}{2}$	$\frac{3}{2}$	-1	-2

where we assume a to be real and positive. None of the arguments below are qualitatively changed if we consider the linear function $F = aS$ as in the original Ref. [19]. The reason we take a quadratic function is to ensure positiveness of the gauge kinetic term. The mass dimensions of the fields and parameters are summarized in Table 1.

The equations of motion for the above model are

$$D_M \left\{G^{MN}, S^2\right\} - \frac{1}{N} \operatorname{Tr}\left[D_M \left\{G^{MN}, S^2\right\}\right] \mathbf{1}_N = \frac{i}{a}\left(\left[D^N T, T\right] + \left[D^N S, S\right]\right), \tag{2.7}$$

$$D^2 T = \lambda^2 \left\{T, v^2 \mathbf{1}_N - T^2 - S^2\right\} + \xi\, [S, [T, S]], \tag{2.8}$$

$$D^2 S = \lambda^2 \left\{S, v^2 \mathbf{1}_N - T^2 - S^2\right\} + \xi\, [T, [S, T]] - \Omega^2 S + \frac{a}{2}\left\{S, G^2\right\}, \tag{2.9}$$

with $D^2 = D_M D^M$ and $G^2 = G_{MN} G^{MN}$.

The potential V in Eq. (2.3) has a number of discrete vacua,

$$T = v\Lambda, \qquad S = \mathbf{0}_N, \tag{2.10}$$

where $\Lambda^2 = \mathbf{1}_N$. Without loss of generality, by using the SU(N) symmetry, we can diagonalize it as

$$\langle k, N-k\rangle \ \text{vacuum:}\ \Lambda = \operatorname{diag}(\underbrace{1, 1, \ldots, 1}_{k}, \underbrace{-1, -1, \ldots, -1}_{N-k}). \tag{2.11}$$

The 2 vacua $\langle N, 0\rangle$ and $\langle 0, N\rangle$ are SU(N) preserving vacua, which we will use as boundary conditions to obtain background domain wall solutions. All the remaining vacua partially break SU(N). The breaking pattern of SU(N) depends on k as

$$\mathrm{SU}(N) \to S\left[\mathrm{U}(N-k) \times \mathrm{U}(k)\right] \quad (k = 0, 1, \ldots, N). \tag{2.12}$$

In order to find the mass spectrum of each vacuum, let us first replace F by

$$F_\varepsilon \equiv aS^2 + \frac{1}{4g_\varepsilon^2}, \tag{2.13}$$

where g_ε is a fictitious SU(N) gauge coupling. We reproduce the original gauge kinetic term at the limit $g_\varepsilon \to \infty$. Since $S = 0$ at the vacua, we have an ordinary gauge kinetic term with $F_\varepsilon = \frac{1}{4g_\varepsilon^2}$. In the SU($N$) preserving vacua, the masses of T and S are $m_T = \sqrt{2}\lambda v$ and $m_S = \Omega$. The SU(N) gauge fields are unbroken, hence they are massless. The mass spectrum in the $\langle k, N-k\rangle$ vacuum is the following. Similarly to the unbroken vacua, the $k \times k$ and $(N-k) \times (N-k)$ block diagonal elements of T and S are massive with masses $\sqrt{2}\lambda v$ and Ω. The remaining elements in off-diagonal blocks are nothing but the NG zero modes. The corresponding off-diagonal elements of the gauge fields absorb these NG bosons by the standard Higgs mechanism to have mass $\sqrt{2}g_\varepsilon v$, whereas the gauge fields for the unbroken part $S[\mathrm{SU}(k) \times \mathrm{SU}(N-k)]$ remain massless.

Now, let us send $g_\varepsilon \to \infty$ and go back to the original model. The masses of T and S, and also the unbroken gauge fields are not affected by g_ε. Therefore, the block-diagonal components of T

and S maintain their masses $\sqrt{2}\lambda v$ and Ω while those of the gauge fields remain massless. On the other hand, the off-diagonal massive gauge bosons get frozen as their masses become infinitely large $g_\varepsilon v \to \infty$. At the same time, the unbroken $S[\mathrm{U}(k) \times \mathrm{U}(N-k)]$ gauge interaction has the infinitely large coupling constant $g_\varepsilon \to \infty$. We interpret this as a semiclassical manifestation of confining vacua. As we will see below, thanks to the infinite gauge coupling, we can manifestly show that not only the massless gauge fields (Ref. [19]) but also the massive vector bosons localize on/between domain walls.

In short, we insist that there are no light scalar fields in any vacua. They are heavy since their masses are of the 5-dimensional mass scale M_5, which we assume very large compared to 4-dimensional mass scales. Furthermore, the gauge fields are either confined or infinitely heavy. Therefore, no light degrees of freedom exist in any vacua from the 5-dimensional viewpoint. This property should be important for the purpose of constructing phenomenological models, though it is beyond the scope of this paper.

3. Multiple domain walls

3.1. Background domain wall solutions

Let us look for static $y \equiv x^4$-dependent domain wall solutions to Eqs. (2.7)–(2.9). Setting $\partial_\mu = 0$ ($\mu = 0, 1, 2, 3$) and $A_M = 0$, the equations of motion reduce to

$$T'' = -\lambda^2 \left\{T, v^2\mathbf{1}_5 - T^2 - S^2\right\} - \xi\,[S,[T,S]], \tag{3.1}$$

$$S'' = -\lambda^2 \left\{S, v^2\mathbf{1}_5 - T^2 - S^2\right\} - \xi\,[T,[S,T]] + \Omega^2 S. \tag{3.2}$$

We solve these with the boundary conditions

$$T \to \pm v\mathbf{1}_N, \quad S \to 0, \quad \text{as} \quad y \to \pm\infty. \tag{3.3}$$

Note that these equations correspond to a non-Abelian extension of the well-known 2-scalar MSTB model (named after Montonen, Sarker, Trullinger, and Bishop), solutions of which have been studied in detail (Refs. [40–42]). Denoting the solution of the MSTB model as the 1×1 scalar fields $\mathcal{T}(y)$ and $\mathcal{S}(y)$, we can immediately get domain wall solutions of our model by embedding $\mathcal{T}(y)$ and $\mathcal{S}(y)$ into the matrices T and S.

In the MSTB model, 2 types of domain-wall-like solutions are known. The first type is

$$\mathcal{T} = v \tanh v\lambda(y - y_0), \qquad \mathcal{S} = 0, \tag{3.4}$$

which is known to be stable only in the parameter region $\Omega \geq v\lambda$. However, we want the S field to condense inside the domain wall for trapping zero modes of gauge fields by the Ohta–Sakai mechanism (Ref. [19]). Therefore, this solution is not suitable for our purposes.

The second type, which is supported in the parameter region $\Omega < v\lambda$, has 2 different solutions, namely,

$$\mathcal{T} = v \tanh \Omega(y - y_0), \qquad \mathcal{S} = \pm\bar{v}\,\mathrm{sech}\,\Omega(y - y_0), \tag{3.5}$$

where we have defined

$$\bar{v}^2 \equiv v^2 - \frac{\Omega^2}{\lambda^2} > 0. \tag{3.6}$$

The width of the wall is of order Ω^{-1}. One can choose either + or − discrete moduli, but we will use the + solution in what follows for concreteness.[1] The general domain wall solution with the SU(N) unbroken vacua at $y \to \pm\infty$ can be constructed by embedding these into T and S as

$$T = v \tanh \Omega\big(y\mathbf{1}_N - Y\big), \qquad S = \bar{v}\,\mathrm{sech}\,\Omega\big(y\mathbf{1}_N - Y\big), \tag{3.7}$$

where a single $N \times N$ Hermitian matrix Y contains all the free parameters of the solution. Stability of this solution can be shown as follows. First, we can construct the Bogomol'nyi completion of energy density as

$$\begin{aligned}\mathcal{E} = \mathrm{Tr}\bigg[&\Big\{\partial_y T - \frac{\Omega}{2v^3}\big(2v^2 + \bar{\Omega}^2\big)\big(v^2\mathbf{1}_N - T^2\big) + \frac{\Omega}{2v}S^2\Big\}^2 + \Big(\partial_y S + \frac{\Omega}{2v}\big(TS + ST\big)\Big)^2 \\ &+ \frac{\bar{v}^4}{4v^2}(4v^2\lambda^2 - \Omega^2)\Big(\frac{T^2}{v^2} + \frac{S^2}{\bar{v}^2} - \mathbf{1}_N\Big)^2 - \xi\big[T,S\big]^2\bigg] + \mathcal{E}_0,\end{aligned} \tag{3.8}$$

with the bound

$$\mathcal{E} \geq \mathcal{E}_0 \equiv \mathrm{Tr}\left[\frac{\Omega}{v^3}\big(2v^2 + \bar{v}^2\big)\partial_y\Big(v^2 T - \frac{1}{3}T^3\Big) - \frac{\Omega}{v}\partial_y\big(TS^2\big)\right]. \tag{3.9}$$

The bound is saturated when the energy equals the tension of the domain walls,

$$E = \int_{-\infty}^{\infty} dy\, \mathcal{E}_0 = N \times T_W, \quad T_W \equiv \frac{4\Omega}{3}\big(2v^2 + \bar{v}^2\big), \tag{3.10}$$

which implies the BPS equations

$$\partial_y T = \frac{v\Omega}{\bar{v}^2}S^2, \qquad \partial_y S = -\frac{\Omega}{2v}\big(TS + ST\big), \qquad \frac{T^2}{v^2} + \frac{S^2}{\bar{v}^2} = \mathbf{1}_N, \qquad \big[T,S\big] = 0. \tag{3.11}$$

One can easily show that T and S given in Eq. (3.7) solve these BPS equations.

3.2. *Domain walls in the global SU(N) model*

Let us figure out the physical meaning of the parameters contained in the $N \times N$ Hermitian matrix Y. For that purpose, only in this subsection, we will consider the global SU(N) model by turning off the gauge interaction:

$$\tilde{\mathcal{L}}_{\mathrm{B}} = \mathrm{Tr}\big[\partial_M T \partial^M T + \partial_M S \partial^M S\big] - V, \tag{3.12}$$

$$V = \mathrm{Tr}\Big[\lambda^2\big(v^2\mathbf{1}_N - T^2 - S^2\big)^2 + \Omega^2 S^2 - \xi\big[T,S\big]^2\Big]. \tag{3.13}$$

The SU(N) symmetry is now a global symmetry, and T and S in Eq. (3.7) are still solutions. In the global SU(N) model, the parameters in Y are all physical zero modes. Since Y is Hermitian, one can always diagonalize it by an SU(N) transformation as $Y = \mathrm{diag}(y_1, y_2, \ldots, y_{N-1}, y_N)$. We can set $y_1 \leq y_2 \leq \cdots \leq y_N$ without loss of generality. The solution is then of the form

$$T = v\,\mathrm{diag}\big(\tanh\Omega(y - y_1), \ldots, \tanh\Omega(y - y_N)\big), \tag{3.14}$$

$$S = \bar{v}\,\mathrm{diag}\big(\mathrm{sech}\,\Omega(y - y_1), \ldots, \mathrm{sech}\,\Omega(y - y_N)\big). \tag{3.15}$$

[1] This is the main reason for choosing the quadratic function in Eq. (2.6). If $F(S)$ is linear as in the original work Ref. [19], the solution with the minus sign implies the wrong sign for the kinetic term, and leads to instability of gauge interaction.

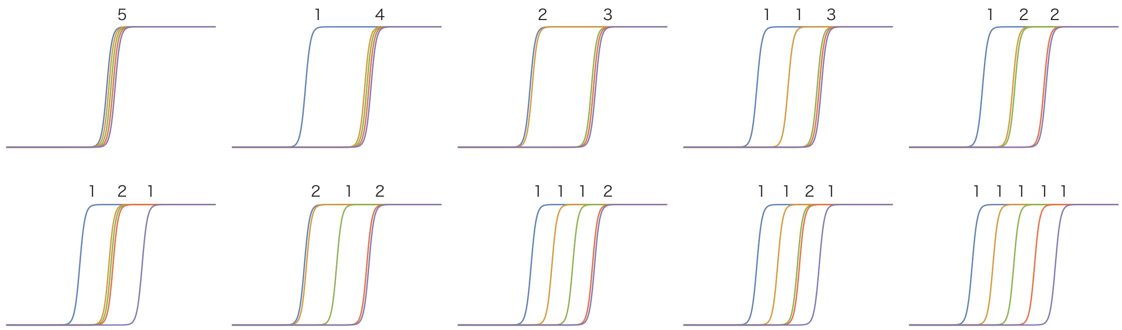

Fig. 1. Amplitudes of the diagonal component of T for 10 different patterns of 5 domain walls in the SU(5) model.

Now, it is manifest that the eigenvalues $\{y_i\}$ correspond to positions of the domain walls in the y-direction. So, we have N domain walls.

Let us next consider a small fluctuation of $Y = Y_0 + \delta Y$ around a given $Y = Y_0$. These fluctuations are zero modes because the shift does not change the energy of the solution. When all the eigenvalues of Y_0 are different, the global SU(N) symmetry is broken to the maximal Abelian subgroup U$(1)^{N-1}$. Therefore $(N^2-1)-(N-1)$ out of N^2 zero modes in Y are NG modes for SU$(N) \to$ U$(1)^{N-1}$. We also have 1 NG mode for the broken translational symmetry and $N-1$ quasi Nambu–Goldstone (qNG) modes associated with the relative distance of N domain walls. In the opposite case, where all the eigenvalues of Y_0 are the same, the N walls are all coincident and the SU(N) symmetry remains intact. There is only 1 NG mode for the broken translational symmetry that corresponds to Tr$[\delta Y]$ and the remaining N^2-1 are qNG. Similar counting can be done for other cases.

To be concrete, let us consider $N = 5$ in the rest of this subsection. Depending on the choice of values of the eigenvalues of Y, we have 10 different patterns of domain walls as shown in Fig. 1. From among those configurations, we concentrate on $Y = Y_0$ with $y_1 = y_2 = y_3 \equiv \mathcal{Y}_3 < \mathcal{Y}_2 \equiv y_4 = y_5$. The domain walls connect the 3 vacua $\langle 0,5\rangle$, $\langle 3,2\rangle$, and $\langle 5,0\rangle$ ordered from left to right. The SU(5) symmetry is intact at the 2 vacua $\langle 0,5\rangle$ and $\langle 5,0\rangle$ but it breaks down to SU(3) $\times$ SU(2) $\times$ U(1) in the middle $\langle 3,2\rangle$ vacuum. The number of NG modes for this partial symmetry breaking is $24-(8+3+1)=12$. This can easily be seen as follows. First, we divide the background configuration into two parts: the SU(5) unbroken part and the SU(5) broken part as

$$\begin{aligned}\begin{pmatrix} T \\ S \end{pmatrix} &= \begin{pmatrix} \begin{pmatrix} \tau_3 \mathbf{1}_3 & 0 \\ 0 & \tau_2 \mathbf{1}_2 \end{pmatrix} \\ \begin{pmatrix} \sigma_3 \mathbf{1}_3 & 0 \\ 0 & \sigma_2 \mathbf{1}_2 \end{pmatrix} \end{pmatrix} \\ &= \mathbf{1}_5 \otimes \begin{pmatrix} \frac{3\tau_3+2\tau_2}{5} \\ \frac{3\sigma_3+2\sigma_2}{5} \end{pmatrix} + \begin{pmatrix} \frac{2}{5}\mathbf{1}_3 & \\ & -\frac{3}{5}\mathbf{1}_2 \end{pmatrix} \otimes \begin{pmatrix} \tau_3 - \tau_2 \\ \sigma_3 - \sigma_2 \end{pmatrix},\end{aligned} \tag{3.16}$$

where we define

$$\tau_i \equiv v \tanh \Omega(y - \mathcal{Y}_i), \quad \sigma_i \equiv \bar{v}\, \mathrm{sech}\, \Omega(y - \mathcal{Y}_i) \quad (i = 2, 3). \tag{3.17}$$

Moreover, an infinitesimal global SU(5) transformation can be parametrized as

$$U_5 = \mathbf{1}_5 + i \begin{pmatrix} \alpha_3 & \tilde{\alpha} \\ \tilde{\alpha}^\dagger & \alpha_2 \end{pmatrix}, \tag{3.18}$$

where α_3 and α_2 are 3×3 and 2×2 infinitesimal Hermitian matrices, with $\mathrm{Tr}\,\alpha_3 + \mathrm{Tr}\,\alpha_2 = 0$, belonging to SU(3) × SU(2) × U(1), while $\tilde{\alpha}$ is a 3×2 complex matrix containing the 12 broken generators. Applying it to Eq. (3.16) we obtain

$$\delta \begin{pmatrix} T \\ S \end{pmatrix} = \begin{pmatrix} \begin{pmatrix} 0 & i\tilde{\alpha}(\tau_3 - \tau_2) \\ -i\tilde{\alpha}^\dagger(\tau_3 - \tau_2) & 0 \end{pmatrix} \\ \begin{pmatrix} 0 & i\tilde{\alpha}(\sigma_3 - \sigma_2) \\ -i\tilde{\alpha}^\dagger(\sigma_3 - \sigma_2) & 0 \end{pmatrix} \end{pmatrix} = \begin{pmatrix} 0 & i\tilde{\alpha} \\ -i\tilde{\alpha}^\dagger & 0 \end{pmatrix} \otimes \begin{pmatrix} \tau_3 - \tau_2 \\ \sigma_3 - \sigma_2 \end{pmatrix}. \tag{3.19}$$

Thus the 12 zero modes in $\tilde{\alpha}$ are nothing but the NG modes. We also have $3^2 + 2^2 - 1 = 12$ qNG modes living in the 3×3 top-left and 2×2 bottom-right corners of δY. Adding the translational zero mode, we again have $12 + 12 + 1 = 25$ zero modes in total. It is important to observe that physics, such as massive spectra and the character of massless modes (NG boson or qNG boson), differ depending on different values of moduli parameters. However, the total number of massless modes (NG and qNG together) remains the same irrespective of the value of moduli parameters (Ref. [24]).

Let us verify the mass spectra and wave functions of each mode by considering small fluctuations around a background configuration. We again take the 3–2 splitting background solution (it is a straightforward task to generalize the following to other cases)

$$T = \begin{pmatrix} \tau_3(y)\mathbf{1}_3 & 0 \\ 0 & \tau_2(y)\mathbf{1}_2 \end{pmatrix} + \begin{pmatrix} t_3(x^\mu, y) & \tilde{t}(x^\mu, y) \\ \tilde{t}(x^\mu, y)^\dagger & t_2(x^\mu, y) \end{pmatrix}, \tag{3.20}$$

$$S = \begin{pmatrix} \sigma_3(y)\mathbf{1}_3 & 0 \\ 0 & \sigma_2(y)\mathbf{1}_2 \end{pmatrix} + \begin{pmatrix} s_3(x^\mu, y) & \tilde{s}(x^\mu, y) \\ \tilde{s}(x^\mu, y)^\dagger & s_2(x^\mu, y) \end{pmatrix}, \tag{3.21}$$

where the first terms on the right-hand sides are the background configurations. The second terms stand for the small fluctuations where t_3, s_3 are 3×3, and t_2, s_2 are 2×2 Hermitian matrices, and $\tilde{t}$, $\tilde{s}$ are 3×2 complex matrices. Linearized equations of motion can be cast into the following form: The diagonal parts are of the form

$$\left(-\partial_M \partial^M - V_i\right) \boldsymbol{t}_i = 0, \quad \boldsymbol{t}_i \equiv \begin{pmatrix} t_i \\ s_i \end{pmatrix}, \tag{3.22}$$

with $i = 3, 2$. Here, $\boldsymbol{t}_i$ is a 2-vector whose components are 3×3 matrices for $i = 3$ and 2×2 matrices for $i = 2$. The 2×2 symmetric matrix Schrödinger potential V_i acts in the 2-component vector space $\boldsymbol{t}_i$. The off-diagonal part has a similar structure:

$$\left(-\partial_M \partial^M - \tilde{V}\right) \tilde{\boldsymbol{t}} = 0, \quad \tilde{\boldsymbol{t}} \equiv \begin{pmatrix} \tilde{t} \\ \tilde{s} \end{pmatrix}, \tag{3.23}$$

where $\tilde{\boldsymbol{t}}$ is a 2-vector whose components are 3×2 matrices, and $\tilde{V}$ is 2×2 symmetric matrix again acting in the 2-vector space $\tilde{\boldsymbol{t}}$. The Schrödinger potentials are

$$V_{i,11} = -2\lambda^2(v^2 - \tau_i^2 - \sigma_i^2) + 4\lambda^2\tau_i^2, \tag{3.24}$$

$$V_{i,12} = V_{i,21} = 4\lambda^2\tau_i\sigma_i, \tag{3.25}$$

$$V_{i,22} = -2\lambda^2(v^2 - \sigma_i^2 - \tau_i^2) + 4\lambda^2\sigma_i^2 + \Omega^2, \tag{3.26}$$

$$\tilde{V}_{11} = \lambda^2(2\tau_3^2 + 2\tau_3\tau_2 + 2\tau_2^2 + \sigma_3^2 + \sigma_2^2 - 2v^2) + \xi(\sigma_3 - \sigma_2)^2, \tag{3.27}$$

$$\tilde{V}_{12} = \tilde{V}_{21} = \lambda^2(\tau_3 + \tau_2)(\sigma_3 + \sigma_2) - \xi(\tau_3 - \tau_2)(\sigma_3 - \sigma_2), \tag{3.28}$$

$$\tilde{V}_{22} = \lambda^2(2\sigma_3^2 + 2\sigma_3\sigma_2 + 2\sigma_2^2 + \tau_3^2 + \tau_2^2 - 2v^2) + \xi(\tau_3 - \tau_2)^2 + \Omega^2. \tag{3.29}$$

Let us expand the fluctuation fields as

$$\boldsymbol{t}_i(x^\mu, y) = \sum_n \begin{pmatrix} \eta_i^{(n)}(x^\mu)\mathbb{u}_{i;1}^{(n)}(y) \\ \eta_i^{(n)}(x^\mu)\mathbb{u}_{i;2}^{(n)}(y) \end{pmatrix} = \sum_n \eta_i^{(n)}(x^\mu) \otimes \mathbb{u}_i^{(n)}(y), \tag{3.30}$$

$$\tilde{\boldsymbol{t}}(x^\mu, y) = \sum_n \begin{pmatrix} \tilde{\eta}_i^{(n)}(x^\mu)\tilde{\mathbb{u}}_{i;1}^{(n)}(y) \\ \tilde{\eta}_i^{(n)}(x^\mu)\tilde{\mathbb{u}}_{i;2}^{(n)}(y) \end{pmatrix} = \sum_n \tilde{\eta}^{(n)}(x^\mu) \otimes \tilde{\mathbb{u}}^{(n)}(y), \tag{3.31}$$

where the basis $\mathbb{u}_i^{(n)} = (\mathbb{u}_{i;1}^{(n)}, \mathbb{u}_{i;2}^{(n)})^t$ and $\tilde{\mathbb{u}}^{(n)} = (\tilde{\mathbb{u}}_{i;1}^{(n)}, \tilde{\mathbb{u}}_{i;2}^{(n)})^t$ are 2-vectors whose components are scalar, and the 4-dimensional effective fields $\eta_3^{(n)}$ and $\eta_2^{(n)}$ are 3×3 and 2×2 Hermitian matrices while $\tilde{\eta}^{(n)}$ is a 3×2 complex matrix. Note that the upper and lower components share the same 4-dimensional effective fields $\eta_i^{(n)}$ and $\tilde{\eta}^{(n)}$. The mass dimensions of the fields are $[\eta] = 1$ and $[\mathbb{u}] = \frac{1}{2}$. In order to figure out the spectrum, it is convenient to define the basis by

$$\left(-\partial_y^2 + V_i\right)\mathbb{u}_i^{(n)} = m_{i,n}^2 \mathbb{u}_i^{(n)}, \qquad \left(-\partial_y^2 + \tilde{V}\right)\tilde{\mathbb{u}}^{(n)} = \tilde{m}_n^2 \tilde{\mathbb{u}}^{(n)}. \tag{3.32}$$

The wave functions of zero modes can be obtained explicitly as

$$\mathbb{u}_i^{(0)} = \frac{N_i}{\Omega}\,\partial_y \begin{pmatrix} \tau_i \\ \sigma_i \end{pmatrix}, \tag{3.33}$$

$$\tilde{\mathbb{u}}^{(0)} = \tilde{N} \begin{pmatrix} \tau_3 - \tau_2 \\ \sigma_3 - \sigma_2 \end{pmatrix}, \tag{3.34}$$

where N_i and $\tilde{N}$ stand for normalization constants whose mass dimensions are $[N_i] = [\tilde{N}] = -1$. Figure 2 shows the wave functions. The former wave function $\mathbb{u}_i^{(0)}$ is given by the y derivative of the background solutions in the diagonal components. This is expected because, e.g., the zero modes in the 3×3 top-left diagonal small matrix are given by $\tau_3 + t_3 = v \tanh \Omega((y - \mathcal{Y}_3)\mathbf{1}_3 + Y_3)$ and $\sigma_3 + s_3 = \bar{v}\,\mathrm{sech}\,\Omega((y - \mathcal{Y}_3)\mathbf{1}_3 + Y_3)$, with Y_3 being an arbitrary 3×3 Hermitian matrix. As usual, the zero mode wave function should be obtained by differentiating the solution in terms of the moduli parameters Y_3. Since Y_3 is a unique matrix appearing in the solution, the Y_3 derivative can be replaced by the y derivative, i.e., Eq. (3.33). The zero mode of Eq. (3.34) is obtained similarly. These fluctuations correspond to the NG bosons associated with SU(5) $\to$ SU(3) $\times$ SU(2) $\times$ U(1), which we can see directly from the infinitesimal transformation given by the off-diagonal elements of Eq. (3.19).

Defining the inner product for 2-component vectors of a function of y as

$$(\mathbb{u}, \mathbb{v}) \equiv \int dy\, \mathbb{u}^t\, \mathbb{v}, \tag{3.35}$$

the normalization factors are determined by the condition $\left(\mathbb{u}_i^{(0)}, \mathbb{u}_i^{(0)}\right) = \left(\tilde{\mathbb{u}}^{(0)}, \tilde{\mathbb{u}}^{(0)}\right) = 1$. We can explicitly evaluate $\tilde{N}$ to give a function of the wall distance $L = |\mathcal{Y}_2 - \mathcal{Y}_3|$ as

$$\frac{1}{\tilde{N}^2} = 4L\left(\frac{\Omega^2}{\lambda^2}\frac{1}{\sinh L\Omega} + v^2 \tanh\frac{L\Omega}{2}\right) - \frac{4\Omega}{\lambda^2}. \tag{3.36}$$

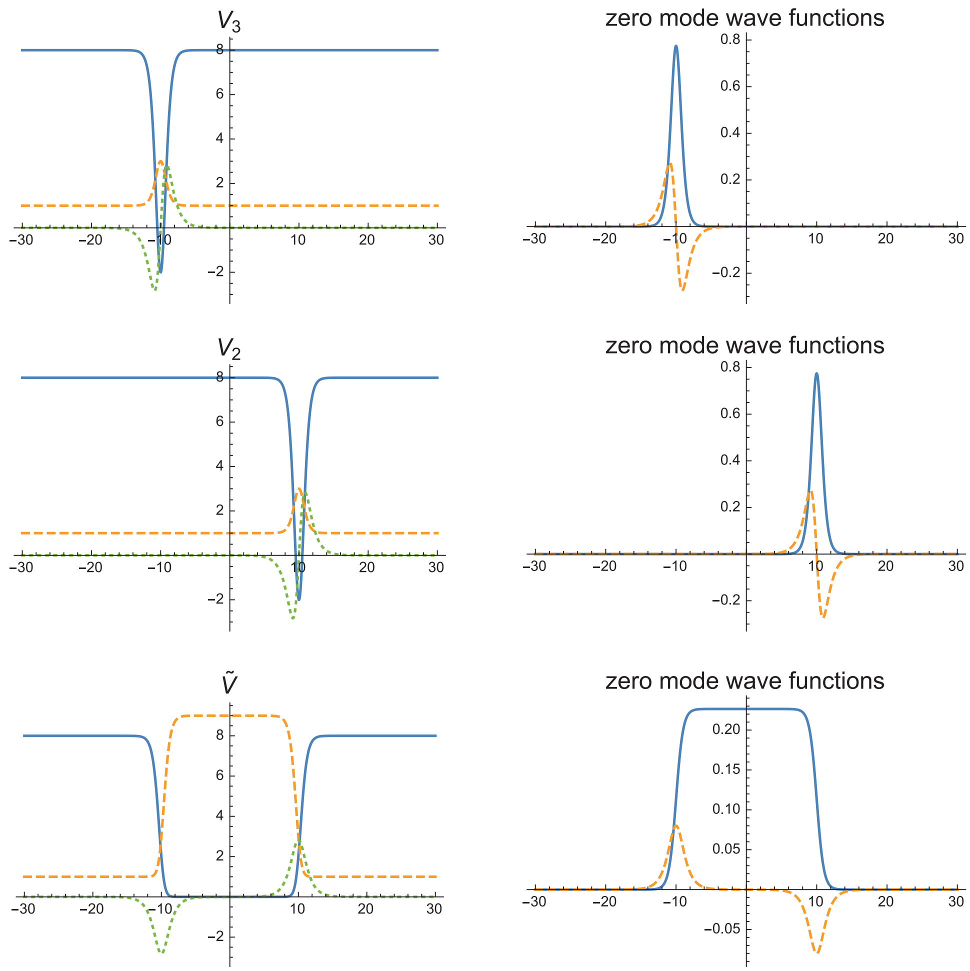

Fig. 2. The Schrödinger potentials V_3, V_2, and $\tilde{V}$ (11 component is the solid line, 22 component is the dashed line, 12 component is the dotted line) are shown in the left panel in the top, middle, and bottom rows, respectively. The corresponding zero mode wave functions $\mathbb{u}_3^{(0)}$, $\mathbb{u}_2^{(0)}$, and $\tilde{\mathbb{u}}^{(0)}$ (the upper component is the solid line and the lower component is the dashed line) are shown in the right panels. The plots are for $\mathcal{Y}_3 = -10$ and $\mathcal{Y}_2 = 10$ with the model parameters $v = \sqrt{2}$, $\lambda = 1$, $\Omega = 1$, and $\xi = 1$.

To understand where the effective fields are localized, let us define the profiles of kinetic terms for zero modes as

$$\rho(\boldsymbol{t}_i^{(0)}; y) = \mathbb{u}_i^{(0)t}\, \mathbb{u}_i^{(0)}, \qquad \rho(\tilde{\boldsymbol{t}}^{(0)}; y) = \tilde{\mathbb{u}}^{(0)t}\, \tilde{\mathbb{u}}^{(0)}, \tag{3.37}$$

with the mass dimension $[\rho] = 1$ (compensating the mass dimension -1 from a y integral). As illustrated by a typical example shown in Fig. 3, the 8 qNGs in $\eta_3^{(0)}(x^\mu)$ are localized on the left three coincident walls while the 3 qNGs in $\eta_2^{(0)}(x^\mu)$ are localized on the right two coincident walls. The profile of the kinetic term for the translational NG mode is a linear combination $(\rho(\boldsymbol{t}_3^{(0)}; y) + \rho(\boldsymbol{t}_2^{(0)}; y))/2$, which has support on both the left and right walls. Finally, $\rho(\tilde{\boldsymbol{t}}^{(0)}; y)$ provides the distribution for the 12 NGs $\tilde{\eta}^{(0)}(x^\mu)$ associated with $SU(5) \to SU(3) \times SU(2) \times U(1)$ spreading between the left and right walls. The reason why $\tilde{\eta}^{(0)}$ localizes between walls is clear. It is because the region between walls is asymptotically close to the vacuum $\langle 3, 2\rangle$ where SU(5) is partially broken. They are called the non-Abelian cloud of the non-Abelian domain wall (Ref. [24]).

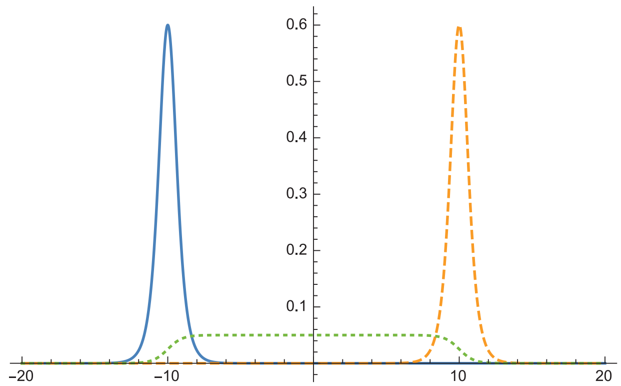

Fig. 3. The profiles of the kinetic terms $\rho(\boldsymbol{t}_3^{(0)}; y)$ (solid line), $\rho(\boldsymbol{t}_2^{(0)}; y)$ (dashed line), and $\rho(\tilde{\boldsymbol{t}}^{(0)}; y)$ (dotted line) are shown for $\mathcal{Y}_3 = -10$ and $\mathcal{Y}_2 = 10$, with the model parameters $v = \sqrt{2}$, $\lambda = 1$, and $\Omega = 1$.

The geometric Higgs mechanism

As long as the SU(5) is a global symmetry, the 25 zero modes are all physical degrees of freedom. However, once the gauge interaction is turned on, the SU(5) becomes a local symmetry. Then the qNGs will remain as the physical zero modes whereas the NGs (except for the translational zero mode) will disappear from the physical spectra because they are absorbed into gauge bosons as their longitudinal components. Thus, the breaking pattern of the gauge symmetry is determined by the domain wall positions in the y-directions. By counting from the leftmost wall, when the number of coincident walls is $(k_1, k_2, \dots, k_n)$ with $\sum_{i=1}^n k_i = 5$, the gauge symmetry is broken as $\mathrm{SU}(5) \to S[\mathrm{U}(k_1) \times \mathrm{U}(k_2) \times \cdots \times \mathrm{U}(k_n)]$. One should note that the Higgs mechanism occurs locally since the would-be NG modes are localized between the split walls. This is the heart of the *geometric Higgs mechanism* that we are going to explain in detail in the subsequent section.

Finally, let us make comments on massive modes. In general, it is not easy to determine the massive modes because the linearized equations of motion (3.22) and (3.23) represent a coupled system of Schrödinger-like equations. Nevertheless, some important information can be derived from the asymptotic values of the potentials,

$$\lim_{y\to\pm\infty} V_3 = \lim_{y\to\pm\infty} V_2 = \lim_{y\to\pm\infty} \tilde{V} = \begin{pmatrix} 4\lambda^2 v^2 & 0 \\ 0 & \Omega^2 \end{pmatrix}. \tag{3.38}$$

First, we see that all the off-diagonal components vanish (see the dotted lines in the left panels of Fig. 2). Therefore, the upper and lower components of $\mathbb{u}_i^{(n)}$ and $\tilde{\mathbb{u}}^{(n)}$ are asymptotically decoupled and become free. They interfere only near the domain walls. Second, we see that there is a common mass gap between massless modes and the continuum spectrum. The mass gap is given by $\min\{2\lambda v, \Omega\}$. Massive modes will be localized between the walls because they are bounded by the quasi-square well $\tilde{V}_{11}$ as is shown in the bottom-left panel (solid line) of Fig. 2.

In order to get a better insight, let us further simplify the global SU(5) model (3.12) and (3.13) by dropping the S field. Then, the simplified model is just an extension of the ϕ^4-type model with the adjoint scalar T only. The background wall solution is given by $T = v \tanh v\lambda(y - Y)$. Let us consider fluctuations like in Eq. (3.20) with $\tau_i = v \tanh v\lambda(y - \mathcal{Y}_i)$ for the 3–2 splitting. The Schrödinger equations for the fluctuations are obtained by just picking up the upper components of Eqs. (3.22) and (3.23). The Schrödinger potential for the diagonal part is $V_{i,11}$ given in Eq. (3.24) with σ_i being

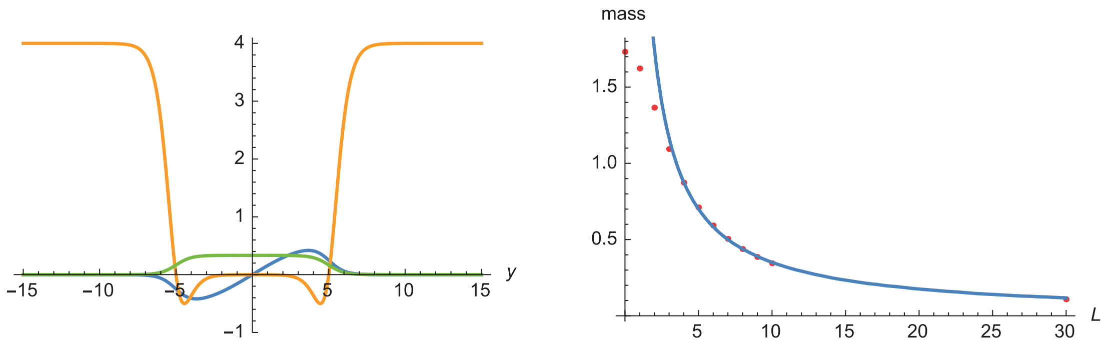

Fig. 4. Left: the Schrödinger potential $\tilde{V}_{11}$ and the wave functions of the zero mode and the first excited mode in the off-diagonal component are shown for $L = 10$. Right: the masses of the first excited modes are plotted with red dots. The solid curve is a numerical fit by $3.5/L$. The parameters are $\lambda = v = 1$.

replaced by 0. This is nothing but the Schrödinger equation for linear fluctuations around a domain wall in the ordinary ϕ^4 model whose spectrum is well known: the lowest modes are massless and the first excited modes have mass $\sqrt{3}\lambda v$. In our reduced model, these modes are the 3×3 and 2×2 matrices in the adjoint representation of SU(3) and SU(2). Note that these modes are blind to whether the SU(5) symmetry is global or local. Similarly, the Schrödinger potential for the off-diagonal components is given by $\tilde{V}_{11}$ in Eq. (3.28) with $\sigma_i \to 0$. Since the existence of zero modes for the off-diagonal components is protected by symmetry, the upper elements of Eq. (3.34) remain as massless modes localized between the domain walls. On the other hand, we need a numerical computation to obtain excited modes since the Schrödinger equation cannot be solved analytically except for 2 extreme limits: the zero-separation limit $|\mathcal{Y}_3 - \mathcal{Y}_2| = 0$, and the infinite-separation limit $\mathcal{Y}_2 \to \infty$ and $\mathcal{Y}_3 \to -\infty$, namely, the vacuum $T = \mathrm{diag}(v, v, v, -v, -v)$. In the former limit, the SU(5) symmetry is unbroken, and therefore both zero modes and excited modes form SU(5) multiplets. This means that t_3, t_2, and $\tilde{t}$ are all on an equal footing, so that the mass of the first excited mode in $\tilde{t}$ should be $\sqrt{3}\lambda v$, as that for the ϕ^4 kink. In the latter limit, the off-diagonal components are the massless NGs. Thus, for the finite separation L, the mass of the first excited mode $\tilde{t}$ is a continuous function, say $\tilde{m}(L)$, of the separation $L = |\mathcal{Y}_3 - \mathcal{Y}_2|$, which asymptotically behaves as $\tilde{m} \to \sqrt{3}\lambda v$ at $L \to 0$ and $\tilde{m} \to 0$ at $L \to \infty$. Indeed, the Schrödinger potential $\tilde{V}_{11}$ at large L is an almost square well whose height is $4\lambda^2 v^2$ and width is L. Therefore, $\tilde{m}$ behaves as $1/L$ at the large L limit; see Fig. 4. In short, the mass spectrum of the off-diagonal element for well-separated domain walls starts from zero and is followed by the massive modes of order $1/L$.

Thus we find that the off-diagonal components have a zero mode and light massive modes of order $1/L$ in the SU(N) global model. Since the zero mode will be eaten by the gauge fields, one anticipates the light massive modes appearing between the domain walls. But we emphasize that this is the case where SU(5) is *global* symmetry. As we will see in later sections, gauging SU(5) will get rid of the off-diagonal zero modes and, at the same time, it increases the masses of massive modes.

4. Mass spectrum on domain walls in the local SU(N) model

Now, we come to main part of this work. Our aim here is to determine the physical spectrum around the background domain walls (3.5) in the gauged model (2.1). The case where all the N domain walls are on top of each other has been intensively studied in Refs. [19,22,23], and the localization mechanism of massless SU(N) gauge fields on the coincident walls is well understood. In contrast, in this work, we will focus on the case where some domain walls are separated from each other. In particular, we will clarify how the massless SU(N) gauge fields acquire nonzero masses, namely, the geometric Higgs mechanism.

We continue to consider the SU(5) model and the 3–2 split domain wall solution (3.7) with $Y = \mathrm{diag}(\mathcal{Y}_3, \mathcal{Y}_3, \mathcal{Y}_3, \mathcal{Y}_2, \mathcal{Y}_2)$, for its phenomenological significance. Extension of our results to both a generic number of walls and arbitrary configurations is straightforward.

4.1. Linearized equations of motion

Let us derive linearized equations of motion for small fluctuations around the 3–2 splitting background solution. The fluctuations in the scalar fields T, S are given in Eqs. (3.20) and (3.21). As this background breaks SU(5) gauge symmetry down to standard model (SM) group $G_{\mathrm{SM}} = \mathrm{SU}(3) \times \mathrm{SU}(2) \times \mathrm{U}(1)_Y$, let us parametrize the surviving symmetry transformations as

$$U_5 = \begin{pmatrix} U_3 & 0 \\ 0 & U_2 \end{pmatrix} \exp\left(i\frac{\alpha T_Y}{2}\right), \quad T_Y = \begin{pmatrix} -\frac{2}{3}\mathbf{1}_3 & 0 \\ 0 & \mathbf{1}_2 \end{pmatrix}, \tag{4.1}$$

where $U_3 \in \mathrm{SU}(3)$, $U_2 \in \mathrm{SU}(2)$, and $\alpha \in \mathrm{U}(1)_Y$. In the following, let us employ the axial gauge in $4+1$ dimensions,

$$A_y = 0. \tag{4.2}$$

There is a residual gauge transformation that depends only on the x^μ-coordinate. Further, let us separate diagonal and off-diagonal degrees of freedom in fluctuations of the gauge fields as

$$A_\mu = 0 + \begin{pmatrix} a_{3\mu} & b_\mu \\ b_\mu^\dagger & a_{2\mu} \end{pmatrix} + a_{1\mu} T_1, \qquad T_1 = \sqrt{\frac{3}{5}} \begin{pmatrix} \frac{1}{3}\mathbf{1}_3 & 0 \\ 0 & -\frac{1}{2}\mathbf{1}_2 \end{pmatrix}, \tag{4.3}$$

where $a_{3\mu}$ is a 3×3 Hermitian traceless matrix and $a_{2\mu}$ is a 2×2 Hermitian traceless matrix, while b_μ is a 3×2 complex matrix. The gauge fields $a_{3\mu}$, $a_{2\mu}$, and $a_{1\mu}$ for SU(3), SU(2), and $\mathrm{U}(1)_Y$ transform under the SM gauge group as

$$a_{3\mu} \to U_3 a_{3\mu} U_3^\dagger + i\partial_\mu U_3 U_3^\dagger, \tag{4.4}$$

$$a_{2\mu} \to U_2 a_{2\mu} U_2^\dagger + i\partial_\mu U_2 U_2^\dagger, \tag{4.5}$$

$$a_{1\mu} \to a_{1\mu} + \sqrt{\frac{5}{3}}\partial_\mu \alpha. \tag{4.6}$$

On the other hand, the b_μ field transforms as

$$b_\mu \to U_3 b_\mu U_2^\dagger \exp\left(-\frac{5i\alpha}{6}\right). \tag{4.7}$$

To investigate the spectrum, we need to write down the linearized equations of motion for each component of Eqs. (3.20), (3.21), and (4.3). Plugging these into equations of motion (2.7)–(2.9), we end up with

$$\partial_M\left(\sigma_\alpha^2 f_\alpha^{MN}\right) = 0, \tag{4.8}$$

$$\left(-\partial_M \partial^M - V_i\right) \boldsymbol{t}_i = 0, \tag{4.9}$$

$$a\partial_M\left(\sigma_+^2 C^{MN}\right) = -\frac{i}{\tilde{N}}\tilde{\mathbb{u}}^{(0)t}\left(\overleftrightarrow{\partial}^N\tilde{\boldsymbol{t}} - \frac{i}{\tilde{N}}b^N\otimes\tilde{\mathbb{u}}^{(0)}\right), \tag{4.10}$$

$$\left(-\partial_M\partial^M - \tilde{V}\right)\tilde{\boldsymbol{t}} = -\frac{i}{\tilde{N}}\left(\partial_M b^M\right)\tilde{\mathbb{u}}^{(0)} - \frac{2i}{\tilde{N}}b^M\otimes\partial_M\tilde{\mathbb{u}}^{(0)}, \tag{4.11}$$

where no sum is taken for $\alpha = 1, 2, 3$ and $i = 3, 2$ in Eqs. (4.8)–(4.9). The linearized field strength is defined as usual by $f_\alpha^{MN} = \partial^M a_\alpha^N - \partial^N a_\alpha^M$, and σ_i $(i = 2, 3)$ is defined in Eq. (3.17). In addition, we have introduced

$$\sigma_1 = \left(\frac{2\sigma_3^2 + 3\sigma_2^2}{5}\right)^{1/2}, \qquad \sigma_+ = \left(\sigma_3^2 + \sigma_2^2\right)^{1/2}, \qquad C^{MN} = \partial^M b^N - \partial^N b^M, \tag{4.12}$$

and $\tilde{\mathbb{u}}^{(0)}$ is given in Eq. (3.34).

4.2. *Diagonal components*

First, we find that the fluctuations a_α^μ $(\mu = 0, 1, 2, 3, \alpha = 1, 2, 3)$ and $\boldsymbol{t}_i$ $(i = 3, 2)$ in the diagonal parts are decoupled from the other fields. In particular, Eq. (4.9) for $\boldsymbol{t}_i$ is exactly the same as Eq. (3.22). Therefore, we have 9 and 4 zero modes in $\boldsymbol{t}_3$ and $\boldsymbol{t}_2$, respectively, whose wave functions have been determined as $\mathbb{u}_3^{(0)}$ and $\mathbb{u}_2^{(0)}$ given in Eq. (3.33).

Let us next investigate the spectrum for the unbroken parts of the gauge fields given in Eq. (4.8). The $N = y$ component in the axial gauge $(b_y = 0)$ is

$$\sigma_\alpha^2\partial_y\partial_\mu a_\alpha^\mu = 0 \quad (\text{no sum for } \alpha), \tag{4.13}$$

and the $N = \nu$ component is

$$\sigma_\alpha^2\partial_\mu f_\alpha^{\mu\nu} + \partial_y(\sigma_\alpha^2\partial^y a_\alpha^\nu) = 0 \quad (\text{no sum for } \alpha). \tag{4.14}$$

We can decompose the gauge field into divergence-free and divergence components as

$$a_\alpha^\mu = a_{\alpha,\text{df}}^\mu + a_{\alpha,\text{d}}^\mu, \quad a_{\alpha,\text{df}}^\mu = (\mathcal{P}_\text{df})^\mu{}_\nu a_\alpha^\nu, \quad a_{\alpha,\text{d}}^\mu = (\mathcal{P}_\text{d})^\mu{}_\nu a_\alpha^\nu, \tag{4.15}$$

where we introduced the projection operators

$$(\mathcal{P}_\text{d})^\mu{}_\nu = \frac{\partial^\mu\partial_\nu}{\partial^2}, \qquad (\mathcal{P}_\text{df})^\mu{}_\nu = \delta_\nu^\mu - \frac{\partial^\mu\partial_\nu}{\partial^2}, \tag{4.16}$$

with the 4-dimensional Laplacian $\partial^2 = \partial_\mu\partial^\mu$. They satisfy the identities

$$\partial_\mu a_{\alpha,\text{df}}^\mu = 0, \quad a_{\alpha,\text{d}}^\mu = \frac{1}{\partial^2}\partial^\mu F_\alpha, \quad F_\alpha = \partial_\nu a_\alpha^\nu. \tag{4.17}$$

The $N = y$ equation tells us that $\partial_y F_\alpha = 0$, so that we have $F_\alpha = F_\alpha(x^\mu)$, which can be gauged away by using the $SU(3)\times SU(2)\times U(1)_Y$ gauge transformation. Then the $N = \nu$ component reads

$$\sigma_\alpha^2\left(\partial^2 - \partial_y^2\right)a_{\alpha,\text{df}}^\nu - (\partial_y\sigma_\alpha^2)\partial_y a_{\alpha,\text{df}}^\nu = 0 \quad (\text{no sum for } \alpha). \tag{4.18}$$

To find the spectrum, let us expand the divergence-free component as

$$a_{\alpha,\text{df}}^\nu = \sum_n w_{\alpha\nu}^{(n)}(x^\mu)f_{a,\alpha}^{(n)}(y) \equiv \sum_n w_{\alpha\nu}^{(n)}(x^\mu)\frac{v_\alpha^{(n)}(y)}{\sigma_\alpha(y)}, \tag{4.19}$$

where $w^{(n)}_{\alpha\nu}(x^\mu)$ is the 4-dimensional gauge field (matrix) and $v^{(n)}_\alpha(y)/\sigma_\alpha(y)$ is its wave function (1 component). The mass dimensions are given by $[w^{(n)}_{\alpha\mu}] = 1$ and $[v^{(n)}_\alpha] = \frac{3}{2}$. The basis of expansion is defined by the Schrödinger equation

$$\left(-\partial_y^2 + V_\alpha\right) v^{(n)}_\alpha = \mu^2_{\alpha,n} v^{(n)}_\alpha, \quad V_\alpha \equiv \frac{1}{\sigma_\alpha}\partial_y^2 \sigma_\alpha = \Omega^2\left(1 - 2\,\mathrm{sech}^2\,\Omega(y - \mathcal{Y}_\alpha)\right), \tag{4.20}$$

where no sum is taken for α.

This Schrödinger-type problem can be cast in the form

$$H_\alpha v^{(n)}_\alpha = \mu^2_{\alpha,n} v^{(n)}_\alpha, \quad H_\alpha = Q^\dagger_\alpha Q_\alpha, \tag{4.21}$$

where we define

$$Q_\alpha = \partial_y - \partial_y \log\sigma_\alpha, \qquad Q^\dagger_\alpha = -\partial_y - \partial_y \log\sigma_\alpha. \tag{4.22}$$

There are two benefits of this expression. First, the Hamiltonian is manifestly positive definite, so that we can be sure that no tachyonic modes exist in the spectrum. Second, the zero mode can be easily found by solving $Qv^{(0)}_\alpha = 0$, which gives

$$v^{(0)}_\alpha(y) = \mathcal{N}_\alpha\,\sigma_\alpha(y), \tag{4.23}$$

where $\mathcal{N}_\alpha$ stands for a normalization constant of the mass dimension $[\mathcal{N}_\alpha] = 0$. The normalization factor $\mathcal{N}_\alpha$ is fixed at $\mathcal{N}_\alpha = 1$ to have a properly normalized field strength $w^{(0)\mu\nu}_\alpha \equiv \partial^\mu w^{(0)\nu}_\alpha - \partial^\nu w^{(0)\mu}_\alpha + i\left[w^{(0)\mu}_\alpha, w^{(0)\nu}_\alpha\right]$. Note that the zero mode wave functions are flat, $\mathcal{N}_\alpha v^{(0)}_\alpha/\sigma_\alpha = 1$; nevertheless, the massless effective gauge fields are localized on the walls thanks to the Ohta–Sakai gauge kinetic function (2.6). The profile of kinetic terms for the zero mode $w^{(0)\mu}_\alpha$ can be read as

$$\rho(w^{(0)}_{\alpha\mu}; y) = a\sigma_\alpha^2 \times \left(\frac{v^{(0)}_\alpha}{\sigma_\alpha}\right)^2 = a(v^{(0)}_\alpha)^2 = a\sigma_\alpha^2 \quad (\text{no sum for } \alpha), \tag{4.24}$$

where the factor $a\sigma_\alpha^2$ reflects the gauge kinetic function (2.6). The mass dimension is $[\rho(w^{(0)}_{\alpha\mu}; y)] = 1$. Figure 5 shows typical profiles of the massless gauge fields. It clearly demonstrates that SU(3) gauge fields localize on the left three coincident walls and SU(2) gauge fields are trapped by the right two coincident walls. The $\mathrm{U}(1)_Y$ gauge fields have support on both the left and right walls.

In general, the Schrödinger equation with the Hamiltonian

$$H = -\partial_y^2 - \frac{c}{\cosh^2(y)} \tag{4.25}$$

has a finite number of discrete bound states. Their energies are given by the textbook formula

$$E_n = -\left(\left(c + \frac{1}{4}\right)^{1/2} - \frac{1}{2} - n\right)^2, \tag{4.26}$$

where n takes nonnegative integer values starting from 0, up to the number for which the expression in the parenthesis is still positive. Given this fact, it is easy to see that for the potential (4.20) there is only the zero mode as a bound state. No other massive discrete bound states exist, while the mass gap between the zero mode and the continuum modes is Ω, which is of order M_5.

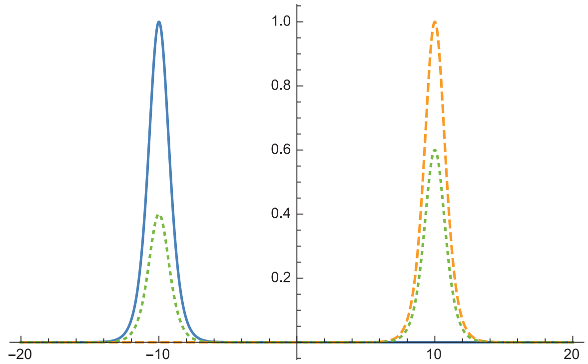

Fig. 5. The profiles of the kinetic terms for $\rho(w^{(0)}_{3\mu};y)$ (solid line), $\rho(w^{(0)}_{2\mu};y)$ (dashed line), and $\rho(w^{(0)}_{1\mu};y)$ (dotted line) are shown for $\mathcal{Y}_3=-10$ and $\mathcal{Y}_2=10$, with the model parameters $v=\sqrt{2}$, $\lambda=1$, and $\Omega=1$.

The effective gauge coupling constants for the effective $\mathrm{SU}(3)\times\mathrm{SU}(2)\times\mathrm{U}(1)_Y$ gauge group can be read as follows. Let us first decompose the gauge kinetic term (2.5) with the fluctuations $a_{i\mu}$ and $b_\mu=0$ in Eq. (4.3):

$$\mathrm{Tr}\left[S^2 G_{MN}G^{MN}\right]=\sigma_3^2\,\mathrm{Tr}\left[f_{3\mu\nu}f_3^{\mu\nu}\right]+\sigma_2^2\,\mathrm{Tr}\left[f_{2\mu\nu}f_2^{\mu\nu}\right]+\left(\frac{\sigma_3^2}{5}+\frac{3\sigma_2^2}{10}\right)f_{1\mu\nu}f_1^{\mu\nu}. \tag{4.27}$$

Integrating this over y, we find the effective gauge couplings:

$$-\frac{1}{2g_3^2}\,\mathrm{Tr}\left[f_{3\mu\nu}f_3^{\mu\nu}\right]-\frac{1}{2g_2^2}\,\mathrm{Tr}\left[f_{2\mu\nu}f_2^{\mu\nu}\right]-\frac{1}{4g_1^2}f_{1\mu\nu}f_1^{\mu\nu}, \tag{4.28}$$

with

$$\frac{1}{g_3^2}=\frac{1}{g_2^2}=\frac{1}{g_1^2}=\frac{4a\bar{v}^2}{\Omega}\equiv\frac{1}{g_5^2}. \tag{4.29}$$

These are the dimensionless gauge coupling constants in $3+1$ dimensions. We see that the effective gauge couplings g_2 and g_3 are given by parameters of the model and that they are equal to each other. The $\mathrm{U}(1)_Y$ coupling e_Y is given by $e_Y=-\sqrt{\frac{3}{20}}g_1$, and is related to g_2 and g_3 as

$$\frac{1}{4e_Y^2}=\frac{2}{3g_3^2}+\frac{1}{g_2^2}=\frac{20a\bar{v}^2}{3\Omega}. \tag{4.30}$$

These relations are identical to the standard SU(5) GUT (grand unification theories) scenario. Hence the prediction of the Weinberg angle at the GUT scale is also the same as the standard SU(5) GUT: $\theta_W=\arctan(2e_Y/g_2)$ is given as $\tan^2\theta_W=3/5$. This purely group-theoretical result arises because of the identical profile of position-dependent gauge couplings for these gauge groups in our simple model. However, we can obtain different profiles for different gauge coupling functions, and a deviation from the standard SU(5) GUT, if we consider models with a more complex structure.

4.3. The geometric Higgs mechanism

Let us next investigate the off-diagonal parts in Eqs. (4.10) and (4.11). These are coupled equations for the fluctuations $\tilde{\boldsymbol{t}}$ and b^M. As we showed in Eq. (3.34), there is a zero mode $\tilde{\eta}^{(0)}(x^\mu)\otimes\tilde{\mathrm{u}}^{(0)}(y)$ in $\tilde{\boldsymbol{t}}$ before coupling to the SU(5) gauge field. We are going to show that this zero mode disappears from the physical spectrum once the gauge interaction is turned on. This is a manifestation of the geometric Higgs mechanism. We continue to use the axial gauge $b_y = 0$.

Let us separate the zero mode and define fields $\bar{\boldsymbol{t}}$ containing only massive modes as

$$\bar{\boldsymbol{t}}(x^\mu, y) = \tilde{\boldsymbol{t}}(x^\mu, y) - \tilde{\eta}^{(0)}(x^\mu) \otimes \tilde{\mathbb{u}}^{(0)}(y), \tag{4.31}$$

where we have defined a 3×2 matrix

$$\tilde{\eta}^{(0)}(x^\mu) = \left(\tilde{\mathbb{u}}^{(0)}(y), \tilde{\boldsymbol{t}}(x^\mu, y)\right). \tag{4.32}$$

Note that the inner product should be taken by means of Eq. (3.35), and remember that the 4-dimensional field $\tilde{\eta}^{(0)}(x^\mu)$ is a 3×2 matrix. Thus, $\bar{\boldsymbol{t}}$ includes only massive modes orthogonal to $\tilde{\mathbb{u}}^{(0)}$. Let us rewrite Eqs. (4.10) and (4.11) by using $\bar{\boldsymbol{t}}$. The $N = \nu$ and $N = y$ components of Eq. (4.10) are of the form

$$a\sigma_+^2 \partial_\mu \tilde{C}^{\mu\nu} + a\partial_y \left(\sigma_+^2 \partial^y \tilde{b}^\nu\right) = -\frac{i}{\tilde{N}} \tilde{\mathbb{u}}^{(0)t}\, \partial^\nu \bar{\boldsymbol{t}} - \frac{\tilde{\mathbb{u}}^{(0)t}\, \tilde{\mathbb{u}}^{(0)}}{\tilde{N}^2} \tilde{b}^\nu, \tag{4.33}$$

$$a\sigma_+^2 \partial^y \partial_\mu \tilde{b}^\mu = \frac{i}{\tilde{N}} \tilde{\mathbb{u}}^{(0)t}\, \overleftrightarrow{\partial^y}\, \bar{\boldsymbol{t}}, \tag{4.34}$$

where we have defined

$$\tilde{b}^\nu(x^\mu, y) = b^\nu(x^\mu, y) + i\tilde{N}\partial^\nu \tilde{\eta}^{(0)}(x^\mu), \tag{4.35}$$

$$\tilde{C}^{\mu\nu} = \partial^\mu \tilde{b}^\nu - \partial^\nu \tilde{b}^\mu. \tag{4.36}$$

Equation (4.11) is also rewritten as

$$-\left(\partial^2 + \partial_y^2 - \tilde{V}\right) \bar{\boldsymbol{t}} = -\frac{i}{\tilde{N}} \left(\partial_\mu \tilde{b}^\mu\right) \otimes \tilde{\mathbb{u}}^{(0)}. \tag{4.37}$$

Now, we are left with Eqs. (4.33), (4.34), and (4.37), and we should note that the off-diagonal scalar zero mode $\tilde{\eta}^{(0)}(x^\mu)$ does not appear alone but is hidden in $\tilde{b}^\nu$. This is nothing but what happens for the standard Higgs mechanism: a massless vector field eats a scalar NG mode and acquires a mass. Indeed, one realizes that Eqs. (4.31) and (4.35) are nothing but the residual gauge transformation $U_5 = U_5(x^\mu) \in \mathrm{SU}(5)$ in the axial gauge $A_y = 0$. We perform the same infinitesimal SU(5) transformation as Eq. (3.19). The only difference here is that the transformation is the gauge transformation. Transforming T and S given in Eqs. (3.20) and (3.21) by U_5 given in Eq. (3.18) with a 3×2 matrix $\tilde{\alpha}(x^\mu)$ of local transformation parameters, we find

$$\tilde{\boldsymbol{t}}(y, x^\mu) \to \tilde{\boldsymbol{t}}'(y, x^\mu) = \tilde{\boldsymbol{t}}(y, x^\mu) - \frac{i}{\tilde{N}} \tilde{\alpha}(x^\mu) \otimes \tilde{\mathbb{u}}^{(0)}(y). \tag{4.38}$$

Similarly, the same infinitesimal gauge transformation of the gauge field given in Eq. (4.3) gives

$$b_\mu(y, x^\mu) \to b'_\mu(y, x^\mu) = b_\mu(y, x^\mu) - \partial_\mu \tilde{\alpha}(x^\mu). \tag{4.39}$$

It is easy to see that gauge transformed $\tilde{\boldsymbol{t}}'$ in Eq. (4.38) and b'_μ in Eq. (4.39) can be identified as $\bar{\boldsymbol{t}}$ in Eq. (4.31) and $\tilde{b}_\mu$ in Eq. (4.35) by choosing the gauge transformation parameter as $\tilde{\alpha}(x^\mu) = -i\tilde{N}\tilde{\eta}^{(0)}(x^\mu)$. We call this choice of gauge the unitary gauge for the geometric Higgs mechanism.

Note also that Eq. (4.34) is redundant because it can be derived from a combination of Eq. (4.33) (after operating ∂_ν) and Eq. (4.37) (after multiplying $\tilde{\mathbb{u}}^{(0)t}$ from the left). Therefore, the spectrum is determined by Eqs. (4.33) and (4.37).

Let us decompose Eqs. (4.33) and (4.37) into divergence and divergence-free parts by applying the projection operators given in Eq. (4.16) as

$$\tilde{b}^\mu = \tilde{b}^\mu_{\rm d} + \tilde{b}^\mu_{\rm df}, \qquad \tilde{b}^\mu_{\rm d} \equiv (\mathcal{P}_{\rm d})^\mu{}_\nu \tilde{b}^\nu, \qquad \tilde{b}^\mu_{\rm df} \equiv (\mathcal{P}_{\rm df})^\mu{}_\nu \tilde{b}^\nu, \tag{4.40}$$

with $\partial_\mu \tilde{b}^\mu_{\rm df} = 0$ due to $(\mathcal{P}_{\rm df})^\mu{}_\nu \partial^\nu = 0$. Now, Eqs. (4.33) and (4.37) are written as

$$a\sigma_+^2 \partial^2 \tilde{b}^\nu_{\rm df} + a\partial_y \left(\sigma_+^2 \partial^y \tilde{b}^\nu_{\rm df}\right) = -\frac{\tilde{\mathbb{u}}^{(0)t}\,\tilde{\mathbb{u}}^{(0)}}{\tilde{N}^2} \tilde{b}^\nu_{\rm df}, \tag{4.41}$$

$$a\partial_y \left(\sigma_+^2 \partial^y \tilde{b}^\mu_{\rm d}\right) = -\frac{i}{\tilde{N}} \tilde{\mathbb{u}}^{(0)t} \left(\partial^\mu \bar{\boldsymbol{t}} - \frac{i}{\tilde{N}} \tilde{b}^\mu_{\rm d} \otimes \tilde{\mathbb{u}}^{(0)}\right), \tag{4.42}$$

$$-\left(\partial_y^2 - \tilde{V}\right) \bar{\boldsymbol{t}} = \partial_\mu \left(\partial^\mu \bar{\boldsymbol{t}} - \frac{i}{\tilde{N}} \tilde{b}^\mu_{\rm d} \otimes \tilde{\mathbb{u}}^{(0)}\right). \tag{4.43}$$

The benefit of this decomposition is that the divergence-free part $\tilde{b}^\mu_{\rm df}$ is decoupled from the other fields. For the time being, we will concentrate on Eq. (4.41) and find the spectrum of $\tilde{b}^\mu_{\rm df}$. To this end, let us expand

$$\tilde{b}^\mu_{\rm df}(x^\nu, y) = \sum_n \beta^{(n)\mu}(x^\nu) \frac{\gamma^{(n)}(y)}{\sigma_+(y)}, \tag{4.44}$$

where $\beta^{(n)}_\mu$ is a 3×2 complex matrix satisfying the divergence-free condition $\partial^\mu \beta^{(n)}_\mu = 0$. The mass dimensions are $[\beta^{(n)}_\mu] = 1$ and $[\gamma^{(n)}] = \frac{3}{2}$. Plugging this into Eq. (4.41), we are lead to

$$\left(\partial^2 + k_n^2\right) \beta^{(n)\nu} = 0, \tag{4.45}$$

$$\left(-\partial_y^2 + \mathcal{V}(y)\right) \gamma^{(n)} = \tilde{\mu}_n^2 \gamma^{(n)}, \tag{4.46}$$

$$\mathcal{V}(y) = \frac{1}{\sigma_+} \partial_y^2 \sigma_+ + \frac{1}{\tilde{N}^2} \frac{\tilde{\mathbb{u}}^{(0)t}\,\tilde{\mathbb{u}}^{(0)}}{a\sigma_+^2}. \tag{4.47}$$

Note that the Schrödinger equation can be written as

$$\tilde{H}\gamma^{(n)} = \tilde{\mu}_n^2 \gamma^{(n)}, \tag{4.48}$$

with the Hamiltonian

$$\tilde{H} = \tilde{Q}^\dagger \tilde{Q} + \frac{1}{\tilde{N}^2} \frac{\tilde{\mathbb{u}}^{(0)t}\,\tilde{\mathbb{u}}^{(0)}}{a\sigma_+^2}, \tag{4.49}$$

where we have defined differential operators

$$\tilde{Q} = \partial_y - \partial_y \log \sigma_+, \qquad \tilde{Q}^\dagger = -\partial_y - \partial_y \log \sigma_+. \tag{4.50}$$

Note that the second term of the Hamiltonian $\tilde{H}$ is positive everywhere if $\mathcal{Y}_3 \neq \mathcal{Y}_2$. It vanishes only when $\mathcal{Y}_3 = \mathcal{Y}_2$ and the Hamiltonian becomes $\tilde{H} = \tilde{Q}^\dagger \tilde{Q}$. In this coincident wall limit, there exists a zero mode that satisfies $\tilde{Q}\gamma^{(0)} = 0$. It is easily solved as

$$\gamma^{(0)} = N_+ \sigma_+, \qquad N_+ = 1. \tag{4.51}$$

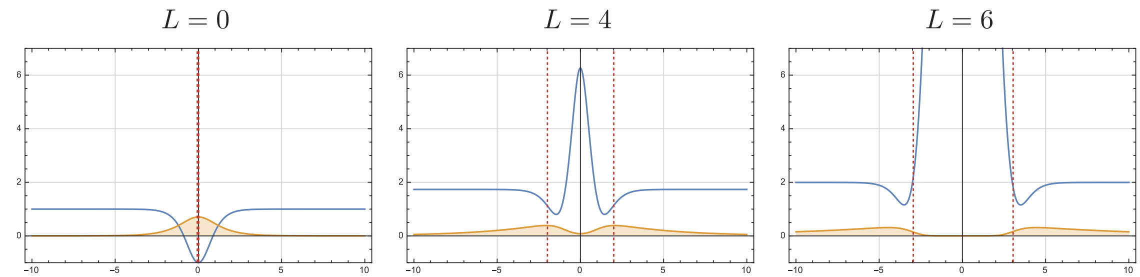

Fig. 6. The Schrödinger potential $\mathcal{V}$ (solid blue line) and the wave function (solid orange shading) of the lightest mode $\gamma^{(0)}$ for $L=0$, $L=4$, and $L=6$ are shown. The model parameters are chosen as $a=1$, $v=\sqrt{2}$, $\lambda=1$, and $\Omega=1$. The red dashed lines show the positions of the domain walls.

The zero mode (4.51) should exist because the SU(5) gauge symmetry is fully unbroken in the coincident wall limit, where not only the diagonal components but also the off-diagonal components of the gauge fields are massless. Since $\tilde{Q}^\dagger\tilde{Q}$ is positive definite, the zero eigenvalue is minimum among all other eigenvalues. When the 3–2 splitting occurs, no matter how small the separation is, the second term of H has a positive contribution to $\tilde{Q}^\dagger\tilde{Q}$. Therefore, the minimum of the spectrum for Eq. (4.48) is positive whenever the walls split. Thus, we conclude that $\tilde{\mu}_n^2>0$ for the 3–2 splitting background. Let us write the lowest mass field as $\beta_\mu=n_\mu\exp(ik^\nu x_\nu)$ with $k^2=\tilde{\mu}_0^2$. The transverse condition $\partial_\mu\beta^\mu=0$ implies $k_\mu n^\mu=0$. Since $k^2=\tilde{\mu}_0^2>0$, there are 3 orthonormal vectors n_a^μ $(a=1,2,3)$. Namely, the vector field $\tilde{b}_{\rm df}^\mu$ orthonormal to k^μ is massive with 3 physical degrees of freedom (2 transverse and 1 longitudinal). This is evidently due to the geometric Higgs mechanism.

Let us obtain the first massive mode. The Schrödinger potential $\mathcal{V}$ for $L=|\mathcal{Y}_2-\mathcal{Y}_3|=0,4,6$ cases are shown in Fig. 6. In the limit with $\Omega L\ll 1$ where the separation is very small, the second term of $\mathcal{V}$ can be treated as a perturbation to the $L=0$ case. Since there exists a localized zero mode $\gamma^{(0)}=\sigma_+$ in the $L=0$ limit, we expect that the bound state remains a massive state as long as $\Omega L\ll 1$. The mass shift is estimated as

$$\tilde{\mu}_0(L)^2=\frac{\left\langle\gamma^{(0)}\middle|\frac{1}{\tilde{N}^2}\frac{\tilde{\mathfrak{u}}^{(0)\dagger}\tilde{\mathfrak{u}}^{(0)}}{a\sigma_+^2}\middle|\gamma^{(0)}\right\rangle}{\left\langle\gamma^{(0)}\middle|\gamma^{(0)}\right\rangle}=\frac{1}{a\tilde{N}^2\left\langle\gamma^{(0)}\middle|\gamma^{(0)}\right\rangle}$$

$$=\frac{\Omega}{4a\bar{v}^2}\left[4L\left(\frac{\Omega^2}{\lambda^2}\frac{1}{\sinh L\Omega}+v^2\tanh\frac{L\Omega}{2}\right)-\frac{4\Omega}{\lambda^2}\right] \tag{4.52}$$

$$\simeq\frac{2}{3}g_5^2\,\Omega\left(2v^2+\bar{v}^2\right)L^2\quad(\Omega L\ll 1), \tag{4.53}$$

where we have used $\frac{1}{g_5^2}=\frac{4a\bar{v}^2}{\Omega}$ as is obtained in Eq. (4.29), $\left\langle\gamma^{(0)}\middle|\gamma^{(0)}\right\rangle=\frac{4\bar{v}^2}{\Omega}$, and $\tilde{N}$ is given in Eq. (3.36). This approximation is compared with numerically obtained masses in Fig. 7. They nicely match for $\Omega L\ll 1$. This behavior resembles the standard Higgs mechanism that the mass of the vector boson is the product of a gauge coupling and a scalar vacuum expectation value (VEV). The mass formula (4.53) says that the effective VEV is

$$v_{\rm eff}=\left(\frac{2}{3}\Omega\left(2v^2+\bar{v}^2\right)\right)^{1/2}L, \tag{4.54}$$

so that the mass is given by $\tilde{\mu}_0(L)^2=g_5v_{\rm eff}$.

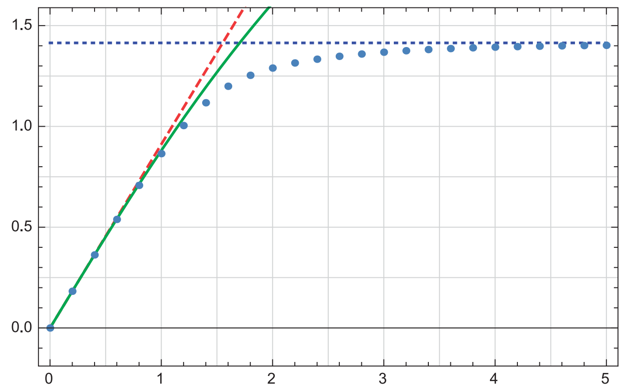

Fig. 7. The mass $\tilde{\mu}_0(L)$ of the lowest discrete massive state of the off-diagonal divergence-free vector field $\tilde{b}^{\mu}_{\rm df}$ as a function of $L = |\mathcal{Y}_3 - \mathcal{Y}_2|$. The dots are numerically obtained, the solid green curve is the analytic approximation given in Eq. (4.52), and the red dashed line is a linear approximation with $k_0(0) = 0$ and $k_0(0.1) = 0.182252$. The model parameters are chosen as $a = 1$, $v = \sqrt{2}$, $\lambda = 1$, and $\Omega = 1$. The blue dotted line shows the mass gap $\left(\Omega^2 + 1/a\right)^{1/2} = \sqrt{2}$.

Note that peculiar phenomena in the geometric Higgs mechanism in our specific model appear in the opposite limit $L\Omega \gg 1$. Indeed, as L is being increased, the bottom of the well is lifted, and a high potential barrier appears at the center of the domain walls. The height of the potential is exponentially large as

$$\mathcal{V}(0) = \frac{\cosh \Omega L - 1}{a} + 2\Omega^2 - 3\Omega^2 \operatorname{sech}^2 \frac{L\Omega}{2} \quad \to \quad \frac{e^{L\Omega}}{2a} \quad \text{as} \quad L \to \infty. \tag{4.55}$$

Therefore, for large separations $\Omega L \gg 1$, as shown in Fig. 6, the massive vector bosons are located not between but on the domain walls, and their masses asymptotically approach the threshold mass $\left(\Omega^2 + 1/a\right)^{1/2}$, which can be read from $\mathcal{V}(\pm\infty) = \Omega^2 + \frac{1 - \operatorname{sech} \Omega L}{a} \sim \Omega^2 + 1/a$. Thus, when the wall separation is large, the mass of the vector boson becomes universal and about $\left(\Omega^2 + 1/a\right)^{1/2}$ irrespective of L, which is of order M_5.

Finally, we have to solve the coupled equations (4.42) and (4.43) for the divergence parts $\tilde{b}^{\mu}_{\rm d}$ and $\bar{\boldsymbol{t}}$. Let us introduce

$$\partial^\mu B \equiv \sigma_+ \partial^\mu \frac{\partial^\nu}{\partial^2} \tilde{b}_\nu = \sigma_+ \tilde{b}^\mu_{\rm d}, \tag{4.56}$$

$$\bar{\boldsymbol{t}}' \equiv \bar{\boldsymbol{t}} - \frac{i}{\tilde{N}} \frac{B}{\sigma_+} \otimes \tilde{\mathbb{u}}^{(0)}. \tag{4.57}$$

There is redundancy such that any function of y can be added to B. Now Eqs. (4.42) and (4.43) are rewritten as

$$\partial^\mu \left[a\sigma_+ \tilde{Q}^\dagger \tilde{Q} B + \frac{i}{\tilde{N}} \tilde{\mathbb{u}}^{(0)t} \bar{\boldsymbol{t}}' \right] = 0, \tag{4.58}$$

$$\left(-\partial_y^2 + \tilde{V}\right) \left(\bar{\boldsymbol{t}}' + \frac{i}{\tilde{N}} \frac{B}{\sigma_+} \otimes \tilde{\mathbb{u}}^{(0)} \right) = \partial^2 \bar{\boldsymbol{t}}', \tag{4.59}$$

where $\tilde{Q}$ and $\tilde{Q}^\dagger$ are defined in Eq. (4.50). The former equation can formally be solved as

$$B = \left(\tilde{Q}^\dagger \tilde{Q}\right)^{-1} \left(\frac{-i}{a\tilde{N}\sigma_+} \tilde{\mathbb{u}}^{(0)t} \bar{\boldsymbol{t}}' + \Lambda(y) \right), \tag{4.60}$$

where $\Lambda(y)$ is an arbitrary function of y that we may set to 0 by absorbing in the redundancy of B. Plugging this into Eq. (4.59), one can eliminate B and we are left with

$$\partial^2 \bar{\boldsymbol{t}}' = \left(-\partial_y^2 + \tilde{V}\right) \left\{ \bar{\boldsymbol{t}}' + \frac{i}{\tilde{N}} \frac{1}{\sigma_+} \left[\left(\tilde{Q}^\dagger \tilde{Q}\right)^{-1} \left(\frac{-i}{a\tilde{N}\sigma_+} \tilde{\mathbb{u}}^{(0)t} \bar{\boldsymbol{t}}' \right) \right] \otimes \tilde{\mathbb{u}}^{(0)} \right\}. \tag{4.61}$$

This formally determines the mass spectrum for $\bar{\boldsymbol{t}}'$ although it is not easily solved analytically. Once we do this, B is determined from Eq. (4.60). Thus, as usual, the divergence part $\tilde{b}^\mu_{\mathrm{d}}$ does not have independent physical degrees of freedom, so that Eq. (4.42) should be regarded as the constraint reducing the 4 polarization degrees of freedom in a massive vector field by 1.

Instead of trying to solve Eq. (4.61), let us understand the spectrum defined by seeing Eq. (4.61) from a different viewpoint. Let us first recall that the second term on the right-hand side of Eq. (4.43) or (4.61) reflects the fact that we gauged SU(5) symmetry of the corresponding mode equation (3.23) in the scalar model considered in Sect. 3.2. As was mentioned at the end of Sect. 3.2, when SU(5) is global symmetry, the 4-dimensional effective fields in $\tilde{\boldsymbol{t}}$ (or $\bar{\boldsymbol{t}}$) are all massless NGs at the infinite wall separation, and they, except for the genuine NGs, are lifted and obtain nonzero mass of order the inverse separation $\sim 1/L$ when the walls are separated by L. This is similar to the standard compactification of the fifth direction to S^1/Z_2 with radius R. In our theory, the extra dimension is infinitely large and our compactification is a posteriori done by the domain walls with the compactification size L. On the other hand, in the S^1/Z_2 model the extra dimension is compact a priori. For simplicity, let us compare the simplest models: the U(1) Goldstone (global) model and the Abelian-Higgs (gauge) model in 5 dimensions compactified by S^1/Z_2 orbifolding,

$$\mathcal{L}_{\mathrm{global}} = |D_M\phi|^2 - \frac{\lambda^2}{4}\left(|\phi|^2 - v^2\right)^2, \tag{4.62}$$

$$\mathcal{L}_{\mathrm{local}} = -\frac{1}{4}F_{MN}F^{MN} + |D_M\phi|^2 - \frac{\lambda^2}{4}\left(|\phi|^2 - v^2\right)^2. \tag{4.63}$$

If the compactification radius R is infinite, the spectrum is 0 and $\sqrt{2}\lambda v$ in the global model, and ev and $\sqrt{2}\lambda v$ in the gauged model. These levels are infinitely degenerate in the 4-dimensional sense. They are split when the compactification radius R is finite. The spectra in the Feynman gauge are split into 0, k/R, $\sqrt{2}\lambda v$, and $\left(2\lambda^2v^2 + (k/R)^2\right)^{1/2}$ in the former model and ev, $\left(e^2v^2 + (k/R)^2\right)^{1/2}$, $\sqrt{2}\lambda v$, and $\left(2\lambda^2v^2 + (k/R)^2\right)^{1/2}$ in the latter model, where k is an integer for the Kaluza–Klein (KK) tower; see Appendix A for details. For our purpose, of understanding Eq. (4.61), we emphasize the fact that the KK tower $\{0, k/R\}$ of the NG modes is shifted to $\{ev, \left(e^2v^2 + (k/R)^2\right)^{1/2}\}$ by gauging U(1) symmetry. Namely, the light modes of order $1/R$ in the global model acquire heavy masses of order ev (the 5-dimensional mass scale) by gauging. This should happen also in our model because the difference between our model and the orbifold model is how to compactify the extra dimension. Remember that the spectrum of $\tilde{\boldsymbol{t}}$ in our scalar model treated in Sect. 3.2 consists of the massless NGs and the massive modes of order $1/L$. When we gauge SU(5) symmetry, the massless NGs are eaten by the geometric Higgs mechanism to give the mass $\tilde{\mu}_0(L)$ (it is of order the fundamental mass scale in 5 dimensions because $\tilde{\mu}_0(L) \to \left(\Omega^2 + 1/a\right)^{1/2}$ for $\Omega L \gg 1$) to the off-diagonal gauge fields. Therefore, the massive modes of order $1/L$ in the scalar model acquire heavy mass of order $\left((1/L)^2 + \tilde{\mu}_0^2\right)^{1/2}$ by gauging. In conclusion, there are no modes below $\tilde{\mu}_0$ in the $\tilde{\boldsymbol{t}}$ channel, and therefore we do not worry about phenomenologically undesired light modes from the off-diagonal elements.

4.4. Field-theoretical D-branes

It is worthwhile pointing out that the number of coincident walls corresponds to the rank of the gauge group preserved by the domain wall configurations. When k domain walls coincide, massless SU(k) gauge fields are localized there. This is quite similar to D-branes in superstring theory. Indeed, in addition to the SU(k) gauge fields, 2 massless scalar fields from T and S in the adjoint representation of SU(k) are localized in our model. This resembles the bosonic component of $\mathcal{N} = 4$ SU(k) vector multiplets appearing at k coincident D3-branes, though we have no fermions and an additional 4 adjoint scalar fields are needed. Furthermore, the mass formula given in Eq. (4.53) for $\Omega L \ll 1$ says that the mass of the lightest vector bosons is proportional to the wall separation L. This is similar to the fact that the massive vector boson on the separated D-branes is proportional to D-brane separation because its origin is F-strings stretching between separated D-branes. Thus, the domain walls in our model with the geometric Higgs mechanism strongly resemble similar mechanisms in D-brane physics.

5. Nonlinear effective Lagrangian for zero modes

In this section, we derive a low-energy effective Lagrangian in the so-called moduli approximation (Ref. [26]), where the moduli parameters of the background solution are promoted to slowly varying fields. In other words, we promote the $N \times N$ matrix of parameters Y in the general solution Eq. (3.7) to 4-dimensional fields $Y \to \Omega^{-1}\mathbf{Y}(x)$ that transform as an adjoint under SU(N). Note that we set $\mathbf{Y}$ to be dimensionless for maintaining simplicity in the following calculations. As a result, the 5-dimensional scalar fields become functions of the effective 4-dimensional moduli fields:

$$T(x,y) = v \tanh\big(\Omega y \mathbf{1}_N - \mathbf{Y}(x)\big), \tag{5.1}$$

$$S(x,y) = \bar{v}\,\mathrm{sech}\big(\Omega y \mathbf{1}_N - \mathbf{Y}(x)\big). \tag{5.2}$$

The goal of this section is to describe effective 4-dimensional dynamics of $\mathbf{Y}(x)$. We present the metric of the moduli space, which gives full nonlinear interaction of moduli fields in a closed form. We limit ourselves to terms with at most 2 derivatives, although we can compute higher-derivative corrections with increasing complexity (Refs. [43,44]).

5.1. Effective Lagrangian in the k_1–k_2 split background

To illustrate our approach, let us first present the effective Lagrangian in a fixed background with a k_1–k_2 split configuration of walls. Furthermore, we will first restrict ourselves to only the leading-order effects in moduli fields to keep the discussion simple. However, in the next subsection, we will present a closed formula for the effective Lagrangian that captures all nonlinear interactions of moduli and works in an arbitrary background.

To pick up the k_1–k_2 background, we assume that $\mathbf{Y}(x)$ is decomposed as

$$\mathbf{Y}(x) = \begin{pmatrix} \mathcal{Y}_{k_1}\mathbf{1}_{k_1} & \mathbf{0}_{k_1\times k_2} \\ \mathbf{0}_{k_2\times k_1} & \mathcal{Y}_{k_2}\mathbf{1}_{k_2} \end{pmatrix} + \begin{pmatrix} \mathbf{Y}_{k_1}(x) & \mathbf{0}_{k_1\times k_2} \\ \mathbf{0}_{k_2\times k_1} & \mathbf{Y}_{k_2}(x) \end{pmatrix}. \tag{5.3}$$

Here, the parameters $\mathcal{Y}_{k_1}$ and $\mathcal{Y}_{k_2}$ are the positions of the k_1 and k_2 walls respectively, while $\mathbf{Y}_{k_1}(x)$ and $\mathbf{Y}_{k_2}(x)$ are fields transforming under the $S[\mathrm{U}(k_1) \times \mathrm{U}(k_2)]$ gauge group. From the point of view of the effective theory we can think of the first part of this decomposition as a "vacuum expectation value" of $\mathbf{Y}(x)$, while the second part represents the fluctuations. The vacuum expectation value $\mathcal{Y}_{k_1} \neq \mathcal{Y}_{k_2}$ is what determines the symmetry-breaking pattern. In this sense, the geometric Higgs mechanism of 5-dimensional theory is similar to an ordinary Higgs mechanism in 4-dimensional theory with $\mathbf{Y}(x)$ playing the role of an adjoint Higgs field.

Notice that off-diagonal components in the second part of the decomposition (5.3) are set to zero. The physical reason is the Higgs mechanism. More precisely, we can always absorb these fields into a definition of the corresponding off-diagonal components of gauge fields by an appropriate gauge transformation. In other words, in the decomposition (5.3) we are assuming the so-called unitary gauge where only physical fields appear.

Next, let us consider the gauge fields. We have established that the wave function of massless gauge fields is flat, hence we can just replace $A_\mu(x,y) \to A_\mu(x)$. However, we also need to decompose the SU(N) gauge fields into the $S[\mathrm{U}(k_1) \times \mathrm{U}(k_2)]$ fields:

$$A_\mu = \begin{pmatrix} a_{k_1\mu} & \mathbf{0}_{k_1\times k_2} \\ \mathbf{0}_{k_2\times k_1} & a_{k_2\mu} \end{pmatrix} + a_{1\mu}T_1, \tag{5.4}$$

$$G^{\mu\nu} = \begin{pmatrix} f_{k_1}^{\mu\nu} & \mathbf{0}_{k_1\times k_2} \\ \mathbf{0}_{k_2\times k_1} & f_{k_2}^{\mu\nu} \end{pmatrix} + f_1^{\mu\nu}T_1, \tag{5.5}$$

where $a_{i\mu}$ and $f_{i\mu\nu}$ ($i = 1, k_1, k_2$) are massless gauge bosons and field strengths of the respective SU(i) gauge groups, while

$$T_1 = \left(\frac{k_1k_2}{2N}\right)^{1/2} \mathrm{diag}\left(\frac{1}{k_1}, \ldots, \frac{1}{k_1}, -\frac{1}{k_2}, \ldots, -\frac{1}{k_2}\right) \tag{5.6}$$

is the hypercharge generator. We do not include the off-diagonal components in the decomposition (5.4) as these represent massive vector bosons and hence, in the spirit of the low-energy limit, we ignore them.

The effective Lagrangian is obtained by inserting all the above decompositions into the full Lagrangian and integrating it over the y-axis. Neglecting higher-than-second powers of moduli fields we get

$$\begin{aligned}\mathcal{L}_{\mathrm{eff}} = &-E - \frac{1}{2g_{k_1}^2}\mathrm{Tr}\big[f_{k_1\mu\nu}f_{k_1}^{\mu\nu}\big] - \frac{1}{2g_{k_2}^2}\mathrm{Tr}\big[f_{k_2\mu\nu}f_{k_2}^{\mu\nu}\big] - \frac{1}{4g_1^2}f_{1\mu\nu}f_1^{\mu\nu} \\ &+ \frac{T_W}{2}\mathrm{Tr}\big[D_\mu\mathbf{Y}_{k_1}D^\mu\mathbf{Y}_{k_1} + D_\mu\mathbf{Y}_{k_2}D^\mu\mathbf{Y}_{k_2}\big] + O\big(\mathbf{Y}_{k_1}^3, \mathbf{Y}_{k_2}^3\big).\end{aligned} \tag{5.7}$$

The contributions without 4-dimensional derivatives sum to the first term $E = NT_W$, which is a constant (topological charge) equal to the total tension of walls given in Eq. (3.10) and has no effect on dynamics. Further, we have the gauge couplings

$$\frac{1}{g_{k_1}^2} = \frac{1}{g_{k_2}^2} = \frac{1}{g_1^2} = \frac{4a\bar{v}^2}{\Omega}. \tag{5.8}$$

This corresponds to those in Eq. (4.29), though here we are considering generic N and k_1 ($k_2 = N - k_1$).

The factor standing in front of the kinetic terms of moduli fields $\mathbf{Y}_{k_1}$ and $\mathbf{Y}_{k_2}$ is equal to $\frac{1}{2}T_W = \frac{1}{2}E/N$ or, in other words, one-half of the tension of a single domain wall. This is to be expected, since the same is true for the translational pseudo-NG zero mode of any domain wall. Indeed, both $\mathbf{Y}_{k_1}$ and $\mathbf{Y}_{k_2}$ contain translational moduli of the respective k_1- and k_2-plets of walls.

The effective Lagrangian (5.7), while a correct 4-dimensional description of the moduli dynamics in the k_1–k_2 split background, has an unsatisfactory feature. It breaks down in the limit $\mathcal{Y}_{k_1} \to \mathcal{Y}_{k_2}$, where the SU($N$) gauge invariance is restored. Indeed, at the coincident point, we have more massless fields than those appearing in Eq. (5.7), namely, off-diagonal components of gauge fields and moduli fields. It would be more appropriate to have an effective theory that can continuously transit from one breaking pattern to another and simultaneously keep track of all fields. Fortunately, this can be done by fully utilizing the moduli approximation as we will see below.

5.2. The extended effective Lagrangian in an arbitrary background

Let us adopt the same ansatz for scalar fields as in Eqs. (5.1)–(5.2). This time, however, we will not assume any particular background and leave the $N \times N$ adjoint moduli fields $\mathbf{Y}(x)$ completely arbitrary. The gauge fields A_μ are given by their zero modes (in axial gauge), which happen to be independent of moduli fields:

$$A_\mu(x,y) = A_\mu(x), \tag{5.9}$$

$$A_y(x,y) = 0. \tag{5.10}$$

Since we are working in an arbitrary background, there is no a priori distinction between unbroken and broken generators. Hence, the formula (5.9) keeps track of all gauge bosons, contrary to our discussion in the previous subsection, where we discarded the off-diagonal massive fields. In what follows, we assume that all $N^2 - 1$ components of A_μ have a flat wave function along the y-axis. This is evidently an approximation, which is forced on us by the fact that we were not able to derive a closed analytic formula for the wave function of massive vector fields. Indeed, we learned in Sect. 4.3 that we can determine $\gamma^{(n)}(y)$ only numerically. If we had such an analytic formula, it would be possible to improve Eq. (5.9) to accommodate for moduli-dependent effects.

The effective Lagrangian is obtained by plugging the ansatz into the 5-dimensional Lagrangian (2.1) and integrating it over the y-axis. When carrying out the calculations, we employ identities that are gathered in Appendix B. The result reads in the following closed form:

$$\mathcal{L}_{\text{eff}} = -E - \frac{1}{2g_5^2}\operatorname{Tr}\big(G_{\mu\nu}G^{\mu\nu}\big) + \operatorname{Tr}\Big\{g\big(\mathcal{L}_{\mathbf{Y}}\big)\big[D_\mu \mathbf{Y}\big]\,D^\mu \mathbf{Y}\Big\}, \tag{5.11}$$

where $\mathcal{L}_{\mathbf{Y}}[\cdot] \equiv [\mathbf{Y}, \cdot]$ is a Lie derivative and where

$$g(\beta) = \frac{4}{\Omega\,\beta^2}\left(v^2\beta\coth(\beta) - \bar{v}^2\beta\cosh(\beta) - \frac{\Omega^2}{\lambda^2}\right). \tag{5.12}$$

This is the main result of this section. The effective Lagrangian (5.11) captures the full nonlinear interaction of moduli fields to all orders and it can be adapted to any background. For example, we can describe the continuous transition from the fully coincident configuration to the k_1–k_2 split configuration by decomposing moduli fields as in Eq. (5.3). In the limit $\mathcal{Y}_{k_1} \to \mathcal{Y}_{k_2}$ we have unbroken SU(N) gauge symmetry and all gauge fields are massless. Once we depart from this point, the off-diagonal components of gauge fields, which are denoted by a $k_1 \times k_2$ complex matrix b_μ, become massive.

In order to compare this with the results in Sect. 4.3, let us consider $N = 5$ and $(k_1, k_2) = (3, 2)$. In the effective Lagrangian, their mass terms arise as the leading term in the expansion in terms of moduli fields of

$$\frac{1}{2g_5^2}\int_{-\infty}^{\infty} dy\,\mathrm{Tr}\Big[\big[A_\mu, T\big]\big[A^\mu, T\big] + \big[A_\mu, S\big]\big[A^\mu, S\big]\Big]$$
$$= \frac{1}{g_5^2}\left\{4v^2 L \tanh\frac{L\Omega}{2} - \frac{4\Omega}{\lambda^2}\left(1 - \frac{L\Omega}{\sinh L\Omega}\right)\right\}\mathrm{Tr}\big[b^\mu b_\mu^\dagger\big] + \cdots, \tag{5.13}$$

where $L \equiv \frac{y_3 - y_2}{\Omega}$ and where the ellipsis points indicate higher-order corrections describing the interaction of b_μ with moduli fields. Now, we can read the mass of a massive gauge boson b_μ,

$$\tilde{\mu}_0^{(\mathrm{eff})}(L)^2 = \frac{1}{g_5^2}\left[4v^2 L \tanh\frac{L\Omega}{2} - \frac{4\Omega}{\lambda^2}\left(1 - \frac{L\Omega}{\sinh L\Omega}\right)\right]. \tag{5.14}$$

Note that this precisely coincides with $\tilde{\mu}_0(L)$ at $\Omega L \ll 1$ given in Eq. (4.53). Thus, the utility of the effective Lagrangian (5.11) is maximal when walls are close to each other. For $\Omega L \gg 1$, this mass, of course, differs from the true mass of b_μ due to the fact that our assumption, the flat wave functions $\gamma^{(0)}$, breaks down.

Note that, as we saw in Eq. (5.7), usually the moduli approximation can deal with only the massless fields and can describe their dynamics at energy scales much below that of the original theory, say M_5 in this work. We should emphasize that the extended effective Lagrangian (5.11) can describe the dynamics of not only the massless fields but also the massive fields. It is quite natural that the mass of a gauge boson is proportional to the wall separation L, hence it can be arbitrarily small. Therefore, the moduli approximation should detect their presence as long as $\Omega L \ll 1$, and indeed Eq. (5.11) can do it. Thus, we have proven with the extended effective Lagrangian (5.11) that the geometric Higgs mechanism occurs at the level of low-energy effective theory.

The third term of the effective Lagrangian (5.11) contains kinetic terms for moduli fields, which exhibit nontrivial self-interaction. This reflects the fact that the moduli space is curved and that the zero modes move along the geodetics (Ref. [26]). The metric of the moduli space can in fact be easily calculated. Let us decompose $\mathbf{Y}$ into generators of $\mathrm{U}(N)$ as $\mathbf{Y} = Y_I T_I = Y_0 \mathbf{1}_5 + Y_a T_a$, where

$$\big[T_a, T_a\big] = i f_{abc} T_c, \qquad \mathrm{Tr}\big[T_a T_b\big] = \frac{1}{2}\delta_{ab}. \tag{5.15}$$

The functions Y_0 and Y_a, $a = 1, \ldots, N^2 - 1$, can be treated as independent zero modes. The metric on the moduli space is then given as the overlap between them:

$$\begin{aligned} g_{IJ} &= 2v^2 \int_{-\infty}^{\infty} dy\,\mathrm{Tr}\Big[\partial_I \tanh\big(\Omega y \mathbf{1}_N - \mathbf{Y}\big)\partial_J \tanh\big(\Omega y \mathbf{1}_N - \mathbf{Y}\big)\Big] \\ &\quad + 2\bar{v}^2 \int_{-\infty}^{\infty} dy\,\mathrm{Tr}\Big[\partial_I \,\mathrm{sech}\big(\Omega y \mathbf{1}_N - \mathbf{Y}\big)\partial_J \,\mathrm{sech}\big(\Omega y \mathbf{1}_N - \mathbf{Y}\big)\Big] \\ &= 2\,\mathrm{Tr}\big[g\big(\mathcal{L}_{\mathbf{Y}}\big)[T_I]\,T_J\big], \end{aligned} \tag{5.16}$$

where $\partial_I Y_J = \delta_{IJ}$ and where $g(\mathcal{L}_{\mathbf{Y}})$ is the same as in Eq. (5.12). Using the identity (B.10) from Appendix B, we can write the metric explicitly as

$$g_{00} = N T_W, \qquad g_{0a} = 0, \tag{5.17}$$

$$g_{ab} = \frac{4}{\Omega}\Big(\big(v^2 - \bar{v}^2\big)\tilde{\mathbf{Y}}^{-2} - v^2 \tilde{\mathbf{Y}}^{-1}\tan^{-1}\big(\tilde{\mathbf{Y}}\big) + \bar{v}^2 \tilde{\mathbf{Y}}^{-1}\sin^{-1}\big(\tilde{\mathbf{Y}}\big)\Big)_{ab}, \tag{5.18}$$

where $\tilde{\mathbf{Y}}$ is an $(N^2-1)\times(N^2-1)$ matrix with elements $\tilde{\mathbf{Y}}_{ab}=f_{abc}Y_c$. With the above metric we can rewrite the third term of $\mathcal{L}_{\rm eff}$ in the compact form

$$\frac{1}{2}g_{IJ}\big(D_\mu Y\big)_I\big(D^\mu Y\big)_J, \tag{5.19}$$

where

$$\big(D_\mu Y\big)_I=\begin{cases} I=0, & \partial_\mu Y_0,\\ I=a, & \partial_\mu Y_a+if_{abc}A_bY_c. \end{cases} \tag{5.20}$$

Although we consider terms up to 2 derivatives only, it is believed that effective dynamics of moduli fields of domain walls can be also captured by the Nambu–Goto-type action or, more generally, as a function of the Nambu–Goto action (Refs. [45–48]). To the best of our knowledge, there seems to be no solid consensus about how to extend the Nambu–Goto action to accommodate non-Abelian symmetry or multi-wall configurations. The results of this section could potentially be relevant for these efforts, especially if they are supplemented by 4-derivative corrections.

6. Conclusions and discussions

In this paper we have presented a (4+1)-dimensional model that gives a framework of dynamical realization of the brane-world model by domain walls, incorporating two core ideas: the semi-classical localization mechanism for gauge fields and the geometric Higgs mechanism using a multi-domain wall background. Since the domain walls interpolate multiple vacua that preserve different subgroups of SU(N), multiple Higgs mechanisms occur locally at the same time. As the domain walls are smooth and continuous solutions of the field equations, the local Higgs mechanisms should be smoothly connected. This is the geometric Higgs mechanism that we have investigated in detail in this work. The off-diagonal vector bosons get nonzero masses by eating the non-Abelian clouds that are localized moduli of the multiple domain wall solutions. In this work, we investigated this phenomenon and evaluated the mass of the vector boson by analyzing the mass spectra from the (4+1)-dimensional viewpoint in Sect. 4. We also confirmed the geometric Higgs mechanism from the perspective of low-energy effective theory on the domain walls in Sect. 5. Through the analysis, we extended the conventional moduli approximation (Ref. [26]) to the theory that naturally includes not only massless modes but also massive modes via the geometric Higgs mechanism, provided the masses are much less than the mass gap of the $(4+1)$-dimensional theory.

Although we have not dealt with the moduli stabilization to find the symmetry breaking of grand unification theories (GUT) in this paper, natural and important application of the geometric Higgs mechanism is, doubtless, to realize the symmetry breaking of GUT dynamically on the domain walls. We will investigate it separately in the subsequent work Ref. [49].

As to the other side of our result, we pointed out a deep similarity between our domain walls and the D-branes in superstring theories. This similarity goes beyond the often-cited connections between field-theoretical solitons and D-branes. The similarities are threefold. First, the number k of coincident walls corresponds to the rank of the special unitary gauge group SU(k). Second, the mass of the massive gauge boson is proportional to the separation of the walls, at least if the separation is sufficiently small. Third, the field content appearing on the k coincident domain walls is a subset of the SU(k) vector multiplet of $\mathcal{N}=4$ supersymmetric

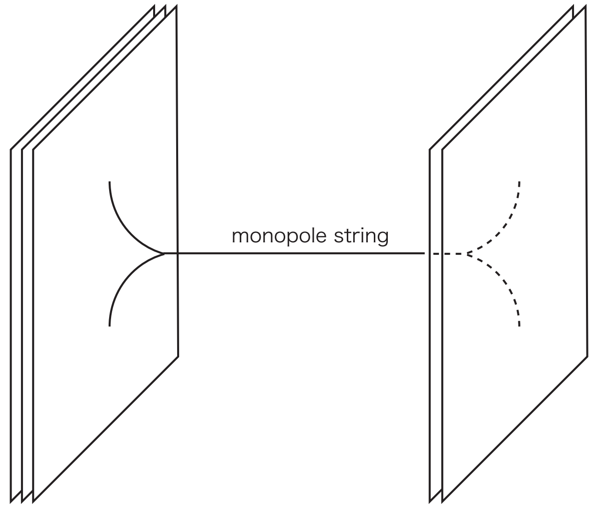

Fig. 8. A schematic depiction of the magnetic monopole from the 5-dimensional point of view as a string stretched between separated domain walls.

Yang–Mills theory that is the low-energy effective theory of k coincident D3-branes. The main reason behind these similarities is the localization of non-Abelian gauge fields, which is caused by the confinement in the bulk realized semiclassically via the field-dependent gauge kinetic term (Ref. [19]).

In this paper, we have not taken SUSY as our guiding principle. However, it may be advantageous to consider 5-dimensional SUSY with 8 supercharges as a master theory. The immediate benefit of implementing SUSY is that a gauge kinetic term as a function of scalar field occurs naturally via the prepotential (Ref. [19]). Further, domain walls are often realized as 1/2 BPS objects, which spontaneously break half of the supercharges. A combination of wall and anti-wall in the background then breaks SUSY entirely (Refs. [50,51]).

Another feature common to most non-Abelian gauge theories is magnetic monopoles, which originate from the breaking of the semisimple gauge group to a subgroup with a U(1) factor. From a phenomenological point of view, monopoles are important in cosmology. In standard Yang–Mills theory in 3+1 dimensions, the magnetic monopoles are 't Hooft–Polyakov-type point-like solitons (Refs. [52,53]). However, in our model monopoles arise as string-like objects, stretched between separated domain walls, as depicted in Fig. 8. The reason is that the asymptotic vacua outside domain walls are SU(N) preserving, while only between the walls the symmetry is broken down to some subgroup, allowing for a nontrivial topology. Let us also remark that this type of configuration has a direct analog in D-strings (Ref. [54]). Detailed study of these observations is the subject of forthcoming work.

Last, in this work we have not discussed gravity for simplicity. However, an interesting direction for future study may be to consider Randall–Sundrum-like theory (Refs. [8,9,55–60]) with multiple branes and to investigate the issues of the cosmological constant and the hierarchy problem there. Another and perhaps more natural option is to employ a position-dependent gravitational constant as a means to localize massless gravitons on multiple domain walls, thus creating the background dynamically. In this setting, it would be interesting to investigate the spectra of graviphotons and fluctuations of domain walls as they are natural candidates for dark matter (for details of massive vector-like dark matter coming from brane oscillations, see Refs. [61,62]). We plan to elaborate on this in the near future.

Acknowledgements

F.B. thanks M. Nitta for useful discussions and comments. F.B. was an international research fellow of the Japan Society for the Promotion of Science, and was supported by Grant-in-Aid for JSPS Fellows, Grant No. 26004750. This work is also supported in part by the Ministry of Education, Culture, Sports, Science (MEXT)-Supported Program for the Strategic Research Foundation at Private Universities "Topological Science", Grant No. S1511006, by the Japan Society for the Promotion of Science (JSPS) Grant-in-Aid for Scientific Research (KAKENHI) Grant Nos. 25400280 (to M.A.), 26800119 and 16H03984 (to M.E.), and 25400241 (to N.S.), and by the Albert Einstein Centre for Gravitation and Astrophysics financed by the Czech Science Agency Grant No. 14-37086G (to F.B.).

Funding

Open Access funding: SCOAP[3].

Appendix A. Kaluza–Klein expansion of the Abelian-Higgs model

Let us consider the Abelian-Higgs model in 5 dimensions:

$$\mathcal{L}_5 = -\frac{1}{4}F_{MN}F^{MN} + |D_M\phi|^2 - \frac{\lambda^2}{4}\left(|\phi|^2 - v^2\right)^2. \tag{A.1}$$

We compactify the fifth direction to S^1/Z_2 with radius R, and we impose periodicity to all fields as $f(y + 2\pi R) = f(y)$. The KK expansions for the scalar and vector fields are given by

$$\phi(x,y) = v + \frac{1}{\sqrt{2\pi R}}\left(\eta^{(0)}(x) + i\sigma^{(0)}(x)\right) + \sum_{k=1}^{\infty}\left(\eta^{(k)}(x) + i\sigma^{(k)}(x)\right)\frac{\cos\frac{k}{R}y}{\sqrt{\pi R}}, \tag{A.2}$$

$$A_\mu(x,y) = \frac{1}{\sqrt{2\pi R}}a_\mu^{(0)}(x) + \frac{1}{\sqrt{\pi R}}\sum_{k=1}^{\infty}a_\mu^{(k)}(x)\cos\frac{k}{R}y, \tag{A.3}$$

$$A_y(x,y) = \frac{1}{\sqrt{\pi R}}\sum_{k=1}^{\infty}a_y^{(k)}(x)\sin\frac{k}{R}y, \tag{A.4}$$

where we have imposed that ϕ and A_μ are even, whereas A_5 is odd for the orbifold parity. Let us write the quadratic Lagrangian by inserting these KK expansions into $\mathcal{L}_5$ and integrating it over y. Then we get

$$-\frac{1}{4}\int_0^{2\pi R}dy\,F_{\mu\nu}F^{\mu\nu} = -\frac{1}{4}f_{\mu\nu}^{(0)}f^{(0)\mu\nu} - \frac{1}{4}\sum_{k=1}^{\infty}f_{\mu\nu}^{(k)}f^{(k)\mu\nu}, \tag{A.5}$$

with $f_{\mu\nu}^{(k)} = \partial_\mu a_\nu^{(k)} - \partial_\nu a_\mu^{(k)}$. We also have

$$-\frac{1}{2}\int_0^{2\pi R}dy\,F_{\mu y}F^{\mu y} = \frac{1}{2}\sum_{k=1}^{\infty}\left(\partial_\mu a_y^{(k)} + \frac{k}{R}a_\mu^{(k)}\right)^2, \tag{A.6}$$

where we have used

$$F_{\mu y} = \frac{1}{\sqrt{\pi R}}\sum_{k=1}^{\infty}\partial_\mu a_y^{(k)}\sin\frac{k}{R}y + \frac{1}{\sqrt{\pi R}}\sum_{k=1}^{\infty}\frac{k}{R}a_\mu^{(k)}\sin\frac{k}{R}y. \tag{A.7}$$

We also have

$$\int_0^{2\pi R} dy\,|D_\mu\phi|^2 = \left(\partial_\mu\eta^{(0)}\right)^2 + (ev)^2\left(a_\mu^{(0)} + \frac{1}{ev}\partial_\mu\sigma^{(0)}\right)^2 + \sum_{k=1}^{\infty}\left\{\left(\partial_\mu\eta^{(k)}\right)^2 + (ev)^2\left(a_\mu^{(k)} + \frac{1}{ev}\partial_\mu\sigma^{(k)}\right)^2\right\}, \tag{A.8}$$

$$\int_0^{2\pi R} dy\,|D_y\phi|^2 = -\sum_{k=1}^{\infty}\left\{\left(\frac{k}{R}\right)^2\eta^{(k)2} + (ev)^2\left(a_y^{(k)} - \frac{1}{ev}\frac{k}{R}\sigma^{(k)}\right)^2\right\}, \tag{A.9}$$

where we have used

$$D_\mu\phi = \frac{1}{\sqrt{2\pi R}}\left\{\partial_\mu\eta^{(0)} + iev\left(a_\mu^{(0)} + \frac{1}{ev}\partial_\mu\sigma^{(0)}\right)\right\} + \frac{1}{\sqrt{\pi R}}\sum_{k=1}^{\infty}\left\{\partial_\mu\eta^{(k)} + iev\left(a_\mu^{(k)} + \frac{1}{ev}\partial_\mu\sigma^{(k)}\right)\right\}\cos\frac{k}{R}y + \cdots, \tag{A.10}$$

$$D_y\phi = -\frac{1}{\sqrt{\pi R}}\sum_{k=1}^{\infty}\left\{\frac{k}{R}\eta^{(k)} - iev\left(a_y^{(k)} - \frac{1}{ev}\frac{k}{R}\sigma^{(k)}\right)\right\}\sin\frac{k}{R}y + \cdots. \tag{A.11}$$

Finally, we have

$$\int_0^{2\pi R} dy\,V = (\lambda v)^2\eta^{(0)2} + (\lambda v)^2\sum_{k=1}^{\infty}\eta^{(k)2}. \tag{A.12}$$

Putting everything together, we find the quadratic Lagrangian

$$\begin{aligned}\mathcal{L}_{\rm 4D}^{(2)} = &-\frac{1}{4}f_{\mu\nu}^{(0)}f^{(0)\mu\nu} + (ev)^2\left(a_\mu^{(0)} + \frac{1}{ev}\partial_\mu\sigma^{(0)}\right)^2 \\ &+ \left(\partial_\mu\eta^{(0)}\right)^2 - (\lambda v)^2\eta^{(0)2} + \sum_{k=1}^{\infty}\left(\partial_\mu\eta^{(k)}\right)^2 - \left[(\lambda v)^2 + \left(\frac{k}{R}\right)^2\right]\eta^{(k)2} \\ &- \frac{1}{4}\sum_{k=1}^{\infty}f_{\mu\nu}^{(k)}f^{(k)\mu\nu} + \frac{1}{2}\sum_{k=1}^{\infty}\left(\partial_\mu a_y^{(k)} + \frac{k}{R}a_\mu^{(k)}\right)^2 \\ &+ \sum_{k=1}^{\infty}(ev)^2\left(a_\mu^{(k)} + \frac{1}{ev}\partial_\mu\sigma^{(k)}\right)^2 - \sum_{k=1}^{\infty}(ev)^2\left(a_y^{(k)} - \frac{1}{ev}\frac{k}{R}\sigma^{(k)}\right)^2.\end{aligned} \tag{A.13}$$

One immediately sees that $\sigma^{(0)}$ and $a_\mu^{(0)}$ appear only in the combination $a_\mu^{(0)} + \frac{1}{ev}\partial_\mu\sigma^{(0)}$, namely, $\sigma^{(0)}$ is absorbed by $a_\mu^{(0)}$, so that $a_\mu^{(0)}$ gets nonzero mass by the ordinary Higgs mechanism. In the $R \to \infty$ limit, the KK tower becomes massless, and indeed each $\sigma^{(k)}$ appears always with $a_\mu^{(k)}$. Namely, the infinite number of 4-dimensional zero modes $\sigma^{(k)}$ are eaten by the infinite number of 4-dimensional massless gauge fields $a_\mu^{(k)}$. It is nothing but the Higgs mechanism in 5 dimensions. In order to untangle the mixing at finite R, let us add the gauge fixing term of the Feynman gauge,

$$\begin{aligned}\mathcal{L}_{\mathrm{F}} &= -\frac{1}{2}\int_0^{2\pi R} dy \left(\partial_M A^M - 2ev\sigma\right)^2 \\ &= -\frac{1}{2}\int_0^{2\pi R} dy \left\{ \frac{1}{\sqrt{2\pi R}}\left(\partial^\mu a_\mu^{(0)} - 2ev\sigma^{(0)}\right) + \sum_{k=1}^{\infty}\left(\partial^\mu a_\mu^{(k)} - \frac{k}{R}a_y^{(k)} - 2ev\sigma^{(k)}\right)\frac{\cos\frac{k}{R}y}{\sqrt{\pi R}} \right\}^2 \\ &= -\frac{1}{2}\left(\partial^\mu a_\mu^{(0)} - 2ev\sigma^{(0)}\right)^2 - \frac{1}{2}\sum_{k=1}^{\infty}\left(\partial^\mu a_\mu^{(k)} - \frac{k}{R}a_y^{(k)} - 2ev\sigma^{(k)}\right)^2, \end{aligned} \tag{A.14}$$

where we have used

$$\partial^\mu A_\mu = \frac{1}{\sqrt{2\pi R}}\partial^\mu a_\mu^{(0)} + \frac{1}{\sqrt{\pi R}}\sum_{k=1}^{\infty}\partial^\mu a_\mu^{(k)}\cos\frac{k}{R}y, \tag{A.15}$$

$$\partial^y A_y = -\frac{1}{\sqrt{\pi R}}\sum_{k=1}^{\infty}\frac{k}{R}a_y^{(k)}\cos\frac{k}{R}y. \tag{A.16}$$

In conclusion, we have

$$\begin{aligned}\mathcal{L}_{\mathrm{4D}}^{(2)} + \mathcal{L}_{\mathrm{F}} &= -\frac{1}{4}f_{\mu\nu}^{(0)}f^{(0)\mu\nu} - \frac{1}{2}\left(\partial_\mu a_\mu^{(0)}\right)^2 + (ev)^2\left(a_\mu^{(0)}\right)^2 \\ &\quad + \left(\partial_\mu\sigma^{(0)}\right)^2 - 2(ev)^2\sigma^{(0)2} + \sum_{k=1}^{\infty}\left\{\left(\partial_\mu\sigma^{(k)}\right)^2 - \left[2(ev)^2 + \left(\frac{k}{R}\right)^2\right]\sigma^{(k)2}\right\} \\ &\quad + \left(\partial_\mu\eta^{(0)}\right)^2 - (\lambda v)^2\eta^{(0)2} + \sum_{k=1}^{\infty}\left\{\left(\partial_\mu\eta^{(k)}\right)^2 - \left[(\lambda v)^2 + \left(\frac{k}{R}\right)^2\right]\eta^{(k)2}\right\} \\ &\quad + \sum_{k=1}^{\infty}\left\{-\frac{1}{4}\sum_{k=1}^{\infty}f_{\mu\nu}^{(k)}f^{(k)\mu\nu} + \frac{1}{2}\left[2(ev)^2 + \left(\frac{k}{R}\right)^2\right]\left(a_\mu^{(k)}\right)^2\right\} \\ &\quad + \frac{1}{2}\sum_{k=1}^{\infty}\left\{\left(\partial_\mu a_y^{(k)}\right)^2 - \left[2(ev)^2 + \left(\frac{k}{R}\right)^2\right]\left(a_y^{(k)}\right)^2\right\}. \end{aligned} \tag{A.17}$$

Now we can read the mass spectrum as $\sqrt{2}ev$, $\left(2(ev)^2 + (k/R)^2\right)^{1/2}$, λv, and $\left((\lambda v)^2 + (k/R)^2\right)^{1/2}$. Thus, all the masses are of order $M_5 = \{\lambda v, ev\}$ or higher than M_5. So, no lighter particles than M_5 exist for any R. This is, of course, because we compactify the fifth direction. Note that the masses shift to 0, k/R, λv, and $\left((\lambda v)^2 + (k/R)^2\right)^{1/2}$ when we turn off the gauge interaction ($e = 0$). The massless mode corresponds to NG for broken global U(1) and the next lightest masses are k/R at large R. In the scalar model (Goldstone model) these KK towers can be very light as R is increased, but once the gauge interaction is turned on, their mass is lifted of order M_5.

Appendix B. Identities for the effective Lagrangian

The calculation of the effective Lagrangians in Sect. 5 is greatly simplified by using a few useful identities described in this appendix.

Let us first consider a generic integral appearing in the kinetic terms of scalar fields, namely,

$$\int_{-\infty}^{\infty} dy\,\mathrm{Tr}\big[D_\mu f(y\mathbf{1}_5 - \mathbf{Y}) D^\mu f(y\mathbf{1}_5 - \mathbf{Y})\big], \tag{B.1}$$

where $\mathcal{L}_{\mathbf{Y}} \equiv [\mathbf{Y}, \cdot]$ is a Lie derivative. The first step in evaluating this integral is to rewrite

$$f(X) = f(\partial_\alpha) e^{\alpha X}\Big|_{a=0}, \tag{B.2}$$

which holds for any f with a Taylor expansion around the origin. Since in all our calculations we deal only with entire functions, such as $\tanh(z)$ or $\mathrm{sech}(z)$, this is clearly satisfied. The second step involves the famous Poincaré identity

$$\delta e^X e^{-X} = \frac{e^{\mathcal{L}_X} - 1}{\mathcal{L}_X}(\delta X). \tag{B.3}$$

This leads to

$$\int_{-\infty}^{\infty} dy\,\mathrm{Tr}\big[D_\mu f(y\mathbf{1}_5 - \mathbf{Y}) D^\mu f(y\mathbf{1}_5 - \mathbf{Y})\big]$$
$$= \int_{-\infty}^{\infty} dy\,\mathrm{Tr}\Big[f(\partial_\alpha) f(\partial_\beta) \exp\left((\alpha+\beta)(y\mathbf{1}_5 - \mathbf{Y})\right) \frac{e^{\alpha\mathcal{L}_{\mathbf{Y}}} - 1}{\mathcal{L}_{\mathbf{Y}}}\big(D_\mu \mathbf{Y}\big) \frac{1 - e^{-\beta\mathcal{L}_{\mathbf{Y}}}}{\mathcal{L}_{\mathbf{Y}}}\big(D^\mu \mathbf{Y}\big)\Big]_{\alpha,\beta=0}. \tag{B.4}$$

Now we can formally shift the integration variable as $y\mathbf{1}_5 - \mathbf{Y} \to y\mathbf{1}_5$. This can be established more rigorously by first diagonalizing the matrix $\exp\left((\alpha+\beta)(y\mathbf{1}_5 - \mathbf{Y})\right)$ and rewriting the integral as the sum of integrals for each diagonal element. We can then shift the integration variable to absorb each diagonal element of $\mathbf{Y}$ separately. Since there is no other y-dependent term in the above integral, this amounts to the shift $y\mathbf{1}_5 - \mathbf{Y} \to y\mathbf{1}_5$, as claimed.

Further, we will use the fact that

$$f(\partial_\alpha) e^{\alpha y}\Big|_{\alpha=0} = f(\partial_\alpha + y)\Big|_{\alpha=0} \tag{B.5}$$

and the properties of the trace to get

$$\int_{-\infty}^{\infty} dy\,\mathrm{Tr}\Big[f(\partial_\alpha + y\mathbf{1}_5) f(\partial_\beta + y\mathbf{1}_5) \frac{e^{\alpha\mathcal{L}_{\mathbf{Y}}} - 1}{\mathcal{L}_{\mathbf{Y}}} \frac{e^{\beta\mathcal{L}_{\mathbf{Y}}} - 1}{\mathcal{L}_{\mathbf{Y}}}\big(D_\mu \mathbf{Y}\big) D^\mu \mathbf{Y}\Big]_{\alpha,\beta=0}. \tag{B.6}$$

This leads to the final result,

$$\int_{-\infty}^{\infty} dy\,\mathrm{Tr}\big[D_\mu f(y\mathbf{1}_5 - \mathbf{Y}) D^\mu f(y\mathbf{1}_5 - \mathbf{Y})\big] = \mathrm{Tr}\Big[g\big(\mathcal{L}_{\mathbf{Y}}\big)\big(D_\mu \mathbf{Y}\big) D^\mu \mathbf{Y}\Big], \tag{B.7}$$

where

$$g(\alpha) \equiv \int_{-\infty}^{\infty} dy \left(\frac{f(y+\alpha) - f(y)}{\alpha} \right)^2. \tag{B.8}$$

Let us also mention an identity relevant to our calculation of the moduli metric. If we decompose an adjoint field Y as $Y = Y_i T_i$, where the T_i are generators of the $\mathrm{SU}(N)$ algebra with the standard normalization

$$[T_i, T_j] = i f_{ijk} T_k, \qquad \mathrm{Tr}[T_i T_j] = \frac{1}{2}\delta_{ij}, \tag{B.9}$$

it is easy to show that

$$g(\mathcal{L}_{\mathbf{Y}})(T_i) = g(i\tilde{\mathbf{Y}})_{ij} T_j, \tag{B.10}$$

where $\tilde{\mathbf{Y}}_{ij} = f_{ijk} Y_k$. This simply comes from Taylor expanding the left side of the identity and repeatedly using the commutation relation for the generators.

References

[1] E. Witten, Nucl. Phys. B **188**, 513 (1981).
[2] S. Dimopoulos and H. Georgi, Nucl. Phys. B **193**, 150 (1981).
[3] N. Sakai, Z. Phys. C **11**, 153 (1981).
[4] S. Dimopoulos, S. Raby, and F. Wilczek, Phys. Rev. D **24**, 1681 (1981).
[5] S. Weinberg, Phys. Rev. D **19**, 1277 (1979).
[6] L. Susskind, Phys. Rev. D **20**, 2619 (1979).
[7] N. Arkani-Hamed, S. Dimopoulos, and G. R. Dvali, Phys. Lett. B **429**, 263 (1998) [arXiv:hep-ph/9803315] [Search INSPIRE].
[8] L. Randall and R. Sundrum, Phys. Rev. Lett. **83**, 3370 (1999) [arXiv:hep-ph/9905221] [Search INSPIRE].
[9] L. Randall and R. Sundrum, Phys. Rev. Lett. **83**, 4690 (1999) [arXiv:hep-th/9906064] [Search INSPIRE].
[10] N. Arkani-Hamed and M. Schmaltz, Phys. Rev. D **61**, 033005 (2000) [arXiv:hep-ph/9903417] [Search INSPIRE].
[11] I. Antoniadis, N. Arkani-Hamed, S. Dimopoulos, and G. R. Dvali, Phys. Lett. B **436**, 257 (1998) [arXiv:hep-ph/9804398] [Search INSPIRE].
[12] V. A. Rubakov and M. E. Shaposhnikov, Phys. Lett. B **125**, 136 (1983).
[13] G. R. Dvali and M. A. Shifman, Phys. Lett. B **396**, 64 (1997); **407**, 452 (1997) [erratum] [arXiv:hep-th/9612128] [Search INSPIRE].
[14] N. Maru and N. Sakai, Prog. Theor. Phys. **111**, 907 (2004) [arXiv:hep-th/0305222] [Search INSPIRE].
[15] C. Germani, Phys. Rev. D **85**, 055025 (2012) [arXiv:1109.3718 [hep-ph]] [Search INSPIRE].
[16] G. R. Dvali, G. Gabadadze, and M. A. Shifman, Phys. Lett. B **497**, 271 (2001) [arXiv:hep-th/0010071] [Search INSPIRE].
[17] S. L. Dubovsky and V. A. Rubakov, Int. J. Mod. Phys. A **16**, 4331 (2001) [arXiv:hep-th/0105243] [Search INSPIRE].
[18] E. K. Akhmedov, Phys. Lett. B **521**, 79 (2001) [arXiv:hep-th/0107223] [Search INSPIRE].
[19] K. Ohta and N. Sakai, Prog. Theor. Phys. **124**, 71 (2010); **127**, 1133 (2012) [erratum] [arXiv:1004.4078 [hep-th]] [Search INSPIRE].
[20] N. Seiberg, Phys. Lett. B **388**, 753 (1996) [arXiv:hep-th/9608111] [Search INSPIRE].
[21] D. R. Morrison and N. Seiberg, Nucl. Phys. B **483**, 229 (1997) [arXiv:hep-th/9609070] [Search INSPIRE].

[22] M. Arai, F. Blaschke, M. Eto, and N. Sakai, Prog. Theor. Exp. Phys. **2013**, 013B05 (2013) [arXiv:1208.6219 [hep-th]] [Search INSPIRE].
[23] M. Arai, F. Blaschke, M. Eto, and N. Sakai, Prog. Theor. Exp. Phys. **2013**, 093B01 (2013) [arXiv:1303.5212 [hep-th]] [Search INSPIRE].
[24] M. Eto, T. Fujimori, M. Nitta, K. Ohashi, and N. Sakai, Phys. Rev. D **77**, 125008 (2008) [arXiv:0802.3135 [hep-th]] [Search INSPIRE].
[25] M. Eto, T. Fujimori, M. Nitta, K. Ohashi, and N. Sakai, J. Phys. Conf. Ser. **222**, 012006 (2010) [arXiv:0912.3590 [hep-th]] [Search INSPIRE].
[26] N. S. Manton, Phys. Lett. B **110**, 54 (1982).
[27] S. M. Carroll and M. Trodden, Phys. Rev. D **57**, 5189 (1998) [arXiv:hep-th/9711099] [Search INSPIRE].
[28] M. Bowick, A. De Felice, and M. Trodden, J. High Energy Phys. **0310**, 067 (2003) [arXiv:hep-th/0306224] [Search INSPIRE].
[29] E. Witten, Nucl. Phys. B **507**, 658 (1997) [arXiv:hep-th/9706109] [Search INSPIRE].
[30] I. I. Kogan, A. Kovner, and M. A. Shifman, Phys. Rev. D **57**, 5195 (1998) [arXiv:hep-th/9712046] [Search INSPIRE].
[31] A. Campos, K. Holland, and U. J. Wiese, Phys. Rev. Lett. **81**, 2420 (1998) [arXiv:hep-th/9805086] [Search INSPIRE].
[32] M. Arai, F. Blaschke, and M. Eto, arXiv:1603.00447 [hep-th] [Search INSPIRE].
[33] M. Arai, F. Blaschke, and M. Eto, arXiv:1612.00306 [hep-th] [Search INSPIRE].
[34] M. Shifman and A. Yung, Phys. Rev. D **70**, 045004 (2004) [arXiv:hep-th/0403149] [Search INSPIRE].
[35] N. Sakai and D. Tong, J. High Energy Phys. **0503**, 019 (2005) [arXiv:hep-th/0501207] [Search INSPIRE].
[36] D. Tong, J. High Energy Phys. **0602**, 030 (2006) [arXiv:hep-th/0512192] [Search INSPIRE].
[37] M. Shifman and A. Yung, Phys. Rev. D **67**, 125007 (2003) [arXiv:hep-th/0212293] [Search INSPIRE].
[38] M. Shifman and A. Yung, Phys. Rev. D **70**, 025013 (2004) [arXiv:hep-th/0312257] [Search INSPIRE].
[39] A. Hanany and D. Tong, J. High Energy Phys. **0307**, 037 (2003) [arXiv:hep-th/0306150] [Search INSPIRE].
[40] C. Montonen, Nucl. Phys. B **112**, 349 (1976).
[41] S. Sarkar, S. E. Trullinger, and A. R. Bishop, Phys. Lett. A **59**, 255 (1976).
[42] H. Ito, Phys. Lett. A **112**, 119 (1985).
[43] M. Eto, T. Fujimori, M. Nitta, K. Ohashi, and N. Sakai, Prog. Theor. Phys. **128**, 67 (2012) [arXiv:1204.0773 [hep-th]] [Search INSPIRE].
[44] M. Eto and Y. Murakami, J. High Energy Phys. **1503**, 078 (2015) [arXiv:1412.7892 [hep-th]] [Search INSPIRE].
[45] E. R. C. Abraham and P. K. Townsend, Phys. Lett. B **291**, 85 (1992).
[46] J. P. Gauntlett, R. Portugues, D. Tong, and P. K. Townsend, Phys. Rev. D **63**, 085002 (2001) [arXiv:hep-th/0008221] [Search INSPIRE].
[47] M. Eto, J. High Energy Phys. **1506**, 160 (2015) [arXiv:1504.00753 [hep-th]] [Search INSPIRE].
[48] M. Eto and K. Hashimoto, Phys. Rev. D **93**, 065058 (2016) [arXiv:1508.00433 [hep-th]] [Search INSPIRE].
[49] M. Arai, F. Blaschke, M. Eto, and N. Sakai, Grand Unified Brane World Scenario [arXiv:1703.00351 [hep-th]] [Search INSPIRE].
[50] N. Maru, N. Sakai, Y. Sakamura, and R. Sugisaka, Nucl. Phys. B **616**, 47 (2001) [arXiv:hep-th/0107204] [Search INSPIRE].
[51] N. Maru, N. Sakai, Y. Sakamura, and R. Sugisaka, Phys. Lett. B **496**, 98 (2000) [arXiv:hep-th/0009023] [Search INSPIRE].
[52] G. 't Hooft, Nucl. Phys. B **79**, 276 (1974).
[53] A. M. Polyakov, JETP Lett. **20**, 194 (1974) [Pisma Zh. Eksp. Teor. Fiz. **20**, 430 (1974)].
[54] D. E. Diaconescu, Nucl. Phys. B **503**, 220 (1997) [arXiv:hep-th/9608163] [Search INSPIRE].
[55] M. Eto, N. Maru, N. Sakai, and T. Sakata, Phys. Lett. B **553**, 87 (2003) [arXiv:hep-th/0208127] [Search INSPIRE].
[56] M. Arai, S. Fujita, M. Naganuma, and N. Sakai, Phys. Lett. B **556**, 192 (2003) [arXiv:hep-th/0212175] [Search INSPIRE].
[57] M. Eto, S. Fujita, M. Naganuma, and N. Sakai, Phys. Rev. D **69**, 025007 (2004) [arXiv:hep-th/0306198] [Search INSPIRE].

[58] M. Eto, N. Maru, and N. Sakai, Nucl. Phys. B **673**, 98 (2003) [arXiv:hep-th/0307206] [Search INSPIRE].
[59] M. Eto and N. Sakai, Phys. Rev. D **68**, 125001 (2003) [arXiv:hep-th/0307276] [Search INSPIRE].
[60] M. Eto, N. Maru, and N. Sakai, Phys. Rev. D **70**, 086002 (2004) [arXiv:hep-th/0403009] [Search INSPIRE].
[61] T. E. Clark, S. T. Love, C. Xiong, M. Nitta, and T. ter Veldhuis, Phys. Rev. D **78**, 115004 (2008) [arXiv:0809.3999 [hep-ph]] [Search INSPIRE].
[62] T. E. Clark, S. T. Love, M. Nitta, T. ter Veldhuis, and C. Xiong, Phys. Lett. B **671**, 383 (2009) [arXiv:0709.4023 [hep-th]] [Search INSPIRE].